ClinchRiverESPHFNPEm Resource

From: Edmondson, Carla <cedmondson@tva.gov>
Sent: Monday, September 18, 2017 10:15 AM
To: Fetter, Allen; Sutton, Mallecia
Subject: [External_Sender] CNL-17-099 CRN RAI Response Number 5 and 6
Attachments: CNL-17-099 CRN RAI Number 5 and 6 Response Regarding Geologic and Seismic Info.pdf

Subject letter has been transmitted to the NRC ML17261A062

CNL-17-099 CRN RAI Response Number 5 and 6

Hard copy to follow via UPS

On behalf of
Joe Shea
VP Nuclear Regulatory Affairs & Support Services

Carla Edmondson
Executive Management Assistant to Joe Shea
423-751-2638

Hearing Identifier: ClinchRiver_ESP_HF_NonPublic
Email Number: 436

Mail Envelope Properties (7D5D7C9A93A2F1418E8AF559D2DAFAF099B98FC3)

Subject: [External_Sender] CNL-17-099 CRN RAI Response Number 5 and 6
Sent Date: 9/18/2017 10:14:50 AM
Received Date: 9/18/2017 10:16:26 AM
From: Edmondson, Carla

Created By: cedmondson@tva.gov

Recipients:
"Fetter, Allen" <Allen.Fetter@nrc.gov>
Tracking Status: None
"Sutton, Mallecia" <Mallecia.Sutton@nrc.gov>
Tracking Status: None

Post Office: TVACHAXCH2.main.tva.gov

Files	**Size**	**Date & Time**
MESSAGE	299	9/18/2017 10:16:26 AM
CNL-17-099 CRN RAI Number 5 and 6 Response Regarding Geologic and Seismic Info.pdf	4671378	

Options
Priority: Standard
Return Notification: No
Reply Requested: No
Sensitivity: Normal
Expiration Date:
Recipients Received:

Tennessee Valley Authority, 1101 Market Street, Chattanooga, TN 37402

CNL-17-099

September 15, 2017

10 CFR 52, Subpart A

ATTN: Document Control Desk
U.S. Nuclear Regulatory Commission
Washington, DC 20555-0001

Clinch River Nuclear Site
NRC Docket No. 52-047

Subject: Response to Request for Additional Information Number 5, Questions 02.05.01-01 and 02.05.01-02, Regarding Basis Geologic and Seismic Information and RAI Number 6, Questions 02.05.04-01 and 02.05.04-02, Regarding Stability of Subsurface Materials and Foundations in Support of Early Site Permit Application for Clinch River Nuclear Site

References:

1. Letter from TVA to NRC, CNL-16-081, "Application for Early Site Permit for Clinch River Nuclear Site," dated May 12, 2016

2. Letter from TVA to NRC, CNL-16-162, "Submittal of Supplemental Information Related to Geologic Characterization Information, Surface Deformation, and Stability of Subsurface Materials and Foundation in Support of Early Site Permit Application for Clinch River Nuclear Site," dated October 21, 2016

3. Letter from TVA to NRC, CNL-16-170, "Submittal of Supplemental Information Related to Vibratory Ground Motion in Support of Early Site Permit Application for Clinch River Nuclear Site," dated October 28, 2016

4. Letter from TVA to NRC, CNL-17-082, "Submittal of Supplemental Information Associated with Site Safety Analysis Report Section 2.5 in Support of the Clinch River Nuclear Site Early Site Permit Application," dated July 3, 2017

5. NRC Electronic Mail, "Issuance of RAI pertaining to Section 2.5.1, Basis Geologic and Seismic Information (RAI Number 5, eRAI-8991)," dated August 1, 2017

6. NRC Electronic Mail, "Issuance of RAI pertaining to Section 2.5.4, Stability of Subsurface Materials and Foundations (RAI Number 6, eRAI-9035)," dated August 1, 2017

By letter dated May 12, 2016 (Reference 1), Tennessee Valley Authority (TVA) submitted an application for an early site permit for the Clinch River Nuclear (CRN) Site in Oak Ridge, TN. By letters dated October 21, 2016 (Reference 2), October 28, 2016 (Reference 3), and July 3, 2017 (Reference 4), TVA provided supplemental information related to geologic characterization information, surface deformation, stability of subsurface materials and foundation, and vibratory ground motion in support of the early site permit application. By electronic mail dated August 1, 2017 (References 5 and 6), Nuclear Regulatory Commission (NRC) issued requests for additional information (RAIs) regarding basic geologic and seismic information and subsurface materials and foundations associated with the CRN Site.

Enclosures 1 and 2 to this letter provide the response to RAI number 5, Questions 02.05.01-01 and 02.05.01-02, respectively, including Site Safety Analysis Report (SSAR) markups. As noted in Reference 5, the response to RAI number 5, Questions 02.05.01-03 through 02.05.01-06, will follow in separate letters. Enclosures 3 and 4 to this letter provide the response to RAI number 6, Questions 02.05.04-01 and 02.05.04-02, respectively, including SSAR markups. The SSAR markups will be incorporated in a future revision of the early site permit application.

There are no new regulatory commitments associated with this submittal. If any additional information is needed, please contact Dan Stout at (423) 751-7642.

I declare under penalty of perjury that the foregoing is true and correct. Executed on this 15th day of September 2017.

Respectfully,

J. W. Shea
Vice President, Nuclear Regulatory Affairs and Support Services

Enclosures:

1. Response to NRC RAI Number 5, Question 02.05.01-01
2. Response to NRC RAI Number 5, Question 02.05.01-02
3. Response to NRC RAI Number 6, Question 02.05.04-01
4. Response to NRC RAI Number 6, Question 02.05.04-02

cc: See page 3

cc: (Enclosures)

A. Fetter, Project Manager, Division of New Reactor Licensing (1 copy)

cc: (without Enclosures)

V. McCree, Executive Director of Operations, USNRC
C. Haney, Regional Administrator, Region II, USNRC
M. Johnson, Deputy Executive Director for Reactor and Preparedness Programs, USNRC
V. Ordaz, Acting Director, Office of New Reactors, USNRC
F. Akstulewicz, Director, Division of New Reactor Licensing, USNRC
J. Colaccino, Branch Chief, Division of New Reactor Licensing, USNRC
M. Sutton, Project Manager, Division of New Reactor Licensing, USNRC
P. Vokoun, Project Manager, Division of New Reactor Licensing, USNRC
T. Dozier, Project Manager, Division of New Reactor Licensing, USNRC
M. M. McIntosh, Regulatory Specialist, Eastern Regulatory Field Office, Nashville District, USACE

Enclosure 1
Response to NRC RAI Number 5, Question 02.05.01-01

NRC RAI 02.05.01-01

Prior Earthquake Effects

SSAR (Rev 0) Section 2.5.1.2.6.6 Prior Earthquake Effects, states that "because it (CRN) is within a zone of elevated seismicity, the CRN site vicinity (25 mile radius) has been extensively evaluated for the presence of paleoseismic features such as those resulting from paleoliquefaction". The SSAR (Rev 0) indicated that this evaluation included geologic field reconnaissance, geologic and geomorphologic mapping, and trench logging of Quaternary terrace deposits along the Douglas Reservoir, Tellico Reservoir and Watts Bar Reservoir. Supplemental information provided in CNL-16-162 and CNL-16-170 provides details regarding the Douglas Reservoir investigation, about 50+ mi to the east of the CRN site.

The presence of paleoliquefaction features is a potentially significant contributor to the demonstration of compliance with 10 CFR 100.23 (c-d). Because insufficient paleoliquifaction feature data were included in the SSAR (Rev 0) sections associated with the Watts Bar and Tellico Reservoirs, please provide details regarding the specific investigation of the paleoliquefaction evaluation within the 25 mile radius of the CRN site. In particular, provide the field reconnaissance information obtained along the Clinch River arm of the Watts Bar and Tellico Reservoirs and provide the associated relevant source documentation.

TVA RAI-02.05.01-01 Response

Field reconnaissance was performed along the shorelines of the Watts Bar and Tellico Reservoirs during geologic investigations to support the Clinch River Nuclear Site Early Site Permit Application. SSAR Subsections 2.5.1.2.6.6, “Prior Earthquake Effects,” and 2.5.3.2, “Geological Evidence, or Absence of Evidence, for Surface Deformation,” are being supplemented with information to describe the results of the field reconnaissance along the shorelines of the Watts Bar and Tellico Reservoirs. The SSAR markups will be incorporated in a future revision of the early site permit application.

Enclosure 1
Response to NRC RAI Number 5, Question 02.05.01-01

SSAR Markups

SSAR Subsection 2.5.1.2.6.6 is being revised as indicated. Underlines indicates text to be added. Strikethroughs indicates text to be deleted.

2.5.1.2.6.6 Prior Earthquake Effects

As described in Subsections 2.5.2 and 2.5.3, the CRN Site is located within a broad zone of elevated activity of historically low-magnitude seismicity that comprises the ETSZ, which is the second most active seismic zone in the eastern United States after the New Madrid seismic zone described in Subsection 2.5.2.2.5). Instrumentally located epicenters in the ETSZ indicate that the majority of earthquake hypocenters are located in the basement rocks beneath the Appalachian fold-thrust belt. Because it is within a zone of elevated seismicity, the CRN site vicinity (25 mile radius) has been extensively evaluated for the presence of paleoseismic features, such as those resulting from paleoliquefaction (see Subsection 2.5.3.2).

An investigation into the presence of paleoliquefaction features within the CRN Site and site vicinity included literature review, geologic field reconnaissance, geologic and geomorphologic mapping, and trench logging of Quaternary terrace deposits along the Douglas Reservoir, Tellico Reservoir and Watts Bar Reservoir. The results of the investigation reveal that while several researchers have identified potential paleoseismic features around the Douglas Reservoir, the origin and interpretation of these features is unclear (as described in Subsection 2.5.3.1.2). Geologic field reconnaissance along the Clinch River arm of the Watts Bar Reservoir and along Tellico Reservoir did not identify ~~any~~ evidence for paleoseismic features (see Subsection 2.5.3.2).

In addition to paleoseismic features, landslides or unstable hillsides or mountain sides can be indicators of past earthquake activity. As described in Subsection 2.5.3 an evaluation of landslide incidence and susceptibility maps indicate that the CRN Site is located in an area of moderate susceptibility and low incidence (Figure 2.4.9-5). Geologic field reconnaissance, aerial photograph analysis, and slope analysis using high-resolution digital elevation data also reveal no existing landslides or other slump-related hazards at the CRN Site.

Enclosure 1
Response to NRC RAI Number 5, Question 02.05.01-01

SSAR Subsection 2.5.3.2.5 is being revised as indicated. Underlines indicates text to be added. Strikethroughs indicates text to be deleted.

2.5.3.2.5 Evaluation of the Presence or Absence of Surface Deformation along the Clinch River Arm of the Watts Bar Reservoir ~~Longitudinal Terrace Profiles along the Clinch River~~

The evaluation of any potential surface deformation features along the Clinch River arm of the Watts Bar Reservoir included a detailed geomorphic investigation supplemented with focused geologic field reconnaissance along exposed Quaternary fluvial terraces. The acquisition of LiDAR across the CRN site area offered the opportunity to reevaluate the evidence for surface faulting or the absence of surface faulting at the site. Evidence for surface faulting in the Quaternary is often expressed by subtle deformation of geomorphic landforms, including river terraces, and can be delineated using anomalies in longitudinal stream and terrace profiles. The high-resolution LiDAR data (0.5 ft pixel resolution) allowed for detailed mapping of Clinch River terraces across the 5-mi radius site area (Figures 2.5.3-2 and 2.5.3-3) and evaluation of the relative ages of terrace levels using morphological correlation and longitudinal profiling (Figure 2.5.3-4). Analysis of longitudinal profiles of terrace elevations can provide a means to assess irregularities that could be associated with reactivation of faults and possible surface deformation. As such, an investigation of terraces along the Clinch River arm of the Watts Bar Reservoir in the site area was undertaken to evaluate ~~any~~ potential evidence for Quaternary surface deformation (see Figure 2.5.1-25 for geologic field reconnaissance waypoint locations; Figures 2.5.3-2, 2.5.3-3, and 2.5.3-4).

2.5.3.2.5.1 Quaternary Deposits

Holocene through Pleistocene alluvial terrace deposits are mapped along the Clinch River arm of the Watts Bar Reservoir and larger tributary valleys in the site area (Figure 2.5.3-2). Terraces along the Clinch River were delineated using high-resolution LiDAR digital elevation data and were checked during field reconnaissance. In the~~se~~ tributary drainages, Holocene terrace levels are assigned based on geomorphology and relative topographic positions, with Qht0 representing the historical flood plain (now flooded and not shown on maps). Tributary terraces of probable Pleistocene age were not assigned a relative terrace level.

Field reconnaissance of fluvial terrace deposits along the Clinch River arm of the Watts Bar Reservoir revealed subtle variations in soil development between interpreted Pleistocene and Holocene terraces. Soil profiles in the Holocene terraces are predominantly dark yellowish brown silt with some clay. Weak pedologic development in the form of soil mottling and blocky soil structure was evident in some Holocene deposits. Pleistocene terrace deposits evaluated in the CRN Site area consist of massive clayey silt and sandy silt deposits with few interbedded gravel-rich units exposed in cross section. Pleistocene terrace treads are frequently littered with abundant subrounded to rounded gravels located on the terrace surfaces regionally. Soil development on these terraces is moderate with often a bleached “E” horizon and a moderately developed “Bt” horizon. Some buried paleosols were visible in deposits along the reservoir margin. Soil profiles were predominantly yellowish brown to dark brown sandy to clayey silt deposits with trace rounded gravels. The Pleistocene terraces have a notable lack of oxidation and no evidence of potential paleoseismic features including fracturing or paleoliquefaction was observed.

Colluvial (Qc) deposits consist of weathered residuum transported by hillslope processes including slopewash and creep. No landslides were mapped within the site area. Colluvium is deposited at the toe of hillslopes and in hollows on the hillsides. Colluvium mapped in the site area is predominantly Holocene, although Pleistocene deposits are likely present. The thickness and areal extent of colluvial deposits varies significantly dependent on the subsurface bedrock unit. The Rome Formation, which erodes primarily by mechanical weathering, produces abundant colluvial deposits that blanket the lower angle slopes underlain by stratigraphically adjacent units. Alternatively, carbonate deposits, which erode primarily by chemical processes, tend to only produce areally extensive colluvial deposits if they contain a significant percentage of chert, such as the Longview Dolomite. Colluvium was mapped primarily on the basis of topographic expression, and only larger bodies are included in Figure 2.5.3-2.

Holocene alluvium (Qha) deposits occur in hillside gullies and in the principal tributary valleys across the site area (Figure 2.5.3-2). Unit Qha includes channel bottom alluvium and low terrace deposits that are undivided at the scale of mapping. The unit is composed largely of silt, with sand and gravel present in varying amounts dependent on the local bedrock parent material. Holocene alluvial fan (Qhf) deposits are present primarily at the mouths of the larger gullies incised into ridges underlain by the Rome Formation.

Enclosure 1
Response to NRC RAI Number 5, Question 02.05.01-01

New SSAR Subsection 2.5.3.2.7 is being inserted prior to Subsection 2.5.3.3, "Correlation of Earthquakes with Capable Tectonic Sources." Underlines indicates text to be added.

2.5.3.2.7 Evaluation of the Presence or Absence of Surface Deformation along the Tellico Reservoir

Following the construction of the Tellico Dam in the 1970s, Tellico Reservoir flooded the Little Tennessee River. Along 54 km of this river, Delcourt (Reference 2.5.3-24; Reference 2.5.3-68) mapped and developed longitudinal topographic profiles for the modern flood plain (T0) and nine older fluvial terrace surfaces (T1 through T9; Reference 2.5.3-69). This terrace mapping included development of five, 1- to 3-km-long trenches at 10-km intervals perpendicular to the river and descriptions and samples of the terrace depositional units from the trench exposures. Radiocarbon dates were obtained on samples collected from terraces T0 through T2, with age results of 3.5 ka, 15 to 3.5 ka, and approximately 28 ka, respectively (Reference 2.5.3-69). The radiocarbon age of T2 is comparable to dates of 29 to 31 ka of correlative terraces of the Tennessee River at the Watts Bar Nuclear Power Plant (Reference 2.5.3-69). Mills and Delcourt (Reference 2.5.3-69) concluded that these terrace ages indicated peak aggradation of sediment occurred at glacial/interglacial or stadial/interstadial transitions rather than solely during peak-glacial intervals as proposed by King (Reference 2.5.3-70). While no radiocarbon dating was performed for terraces T3 through T9, Mills and Delcourt (Reference 2.5.3-69) postulated that these older terraces formed during similar climatic transitions earlier in the Quaternary.

Terrace surfaces along the flooded Little Tennessee River (Tellico Reservoir) were observed and reviewed as part of the field reconnaissance in an effort to: (1) draw comparisons between these terraces and those observed within and adjacent to Douglas Reservoir, and (2) search for potential paleoliquefaction features. The construction of the Tellico Dam, however, resulted in the flooding of the majority of the mapped terraces of Delcourt (Reference 2.5.3-24), leaving only dissected remnant terraces T6 to T9 exposed in select locations. Below is a report of the observations of these terraces along Tellico Reservoir.

Near the Fort Loudon Dam and along the Little Tennessee River, a sequence of terraces, T6, T7, and T9 (as mapped by Delcourt, Reference 2.5.3-24), was observed (Waypoints 240, 242, 243, Figure 2.5.3-21). The T8 terrace does not appear to be preserved in this area. The T6 and T7 terraces were easily distinguishable by their near-horizontal, planar treads (Figure 2.5.3-22A) with relatively small (approximately 1- to 2-m-high) sharp risers. Extensive exposures of the 4-m-high riser between the T7 and T9 treads include well rounded gravel horizons interbedded with strongly oxidized reddish sandy clay terrace deposits (Figure 2.5.3-22B). T9 terrace deposits appear to be approximately 3 to 4 m thick. Small gravel-rich fans emanating from T9 and deposited on T7 were evident. No evidence of potential paleoseismic features, such as fractures, clastic dikes, or paleoliquefaction, was found in these terrace deposits.

Enclosure 1
Response to NRC RAI Number 5, Question 02.05.01-01

The following references are being added to SSAR Subsection 2.5.3.9. Underlines indicates text to be added.

2.5.3.9 References

2.5.3-68. Delcourt, P.A., Delcourt, H.R., Cridlebaugh, P.A., and Chapman, J., Holocene ethnobotanical and paleoecological record of human impact on vegetation in the Little Tennessee River Valley, Tennessee, U.S.A., *Quaternary Research* 25: 330-349, 1986.

2.5.3-69. Mills, H.M, and Delcourt, P.A., Quaternary geology of the Appalachian Highlands and Interior Low Plateaus, *Quaternary Nonglacial: Conterminous U.S.*, *The Geology of North America,* Geological Society of America K-2: 611-628, 1991.

2.5.3-70. King, P.B., Geology of the Elkton area, Virginia, *U.S. Geological Professional Paper* 230: 82 p, 1950.

Enclosure 1
Response to NRC RAI Number 5, Question 02.05.01-01

Figures 2.5.3-21 and 2.5.3-22 are being added to SSAR Subsection 2.5.3

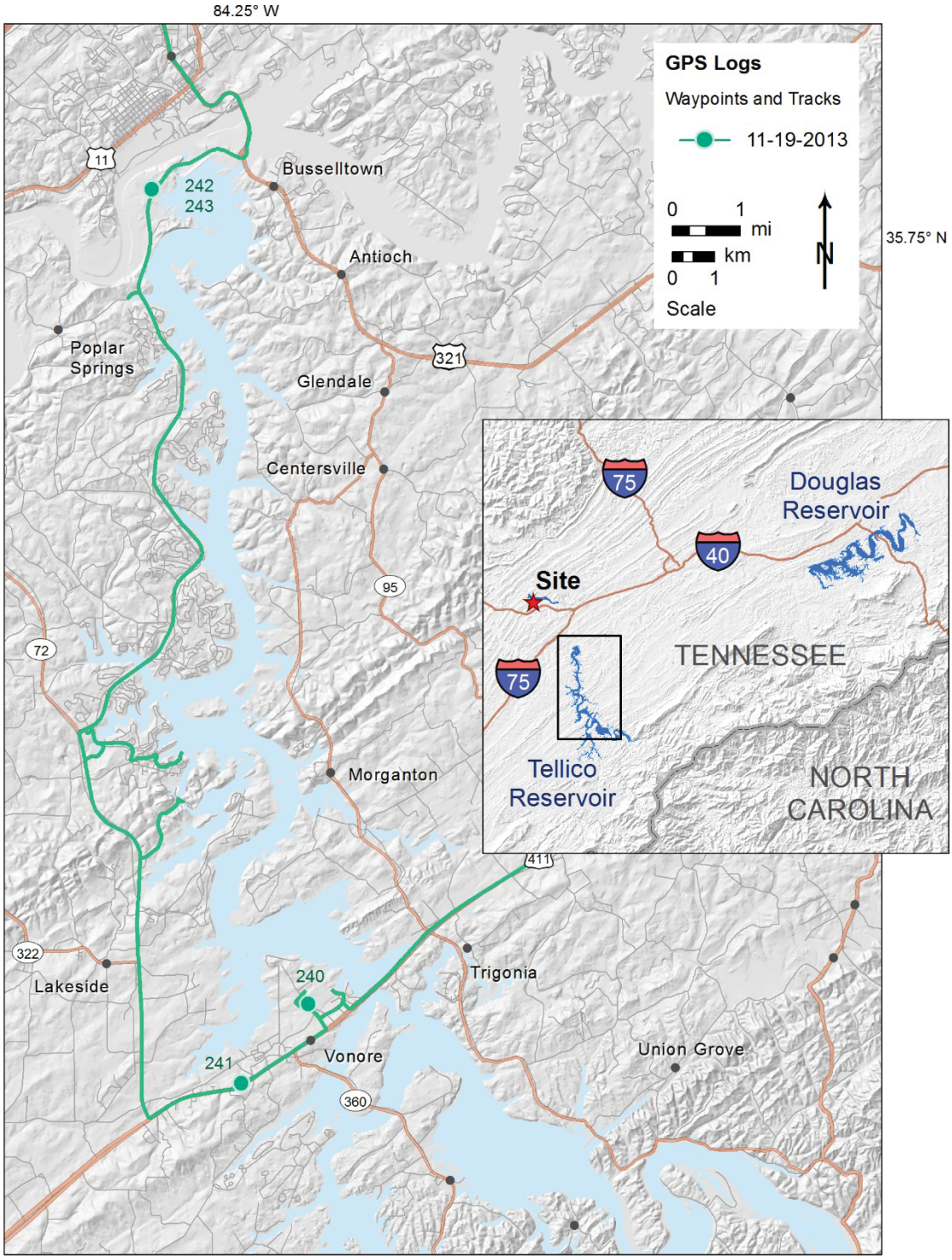

Figure 2.5.3-21. Geologic Field Reconnaissance Waypoint Locations along Tellico Reservoir

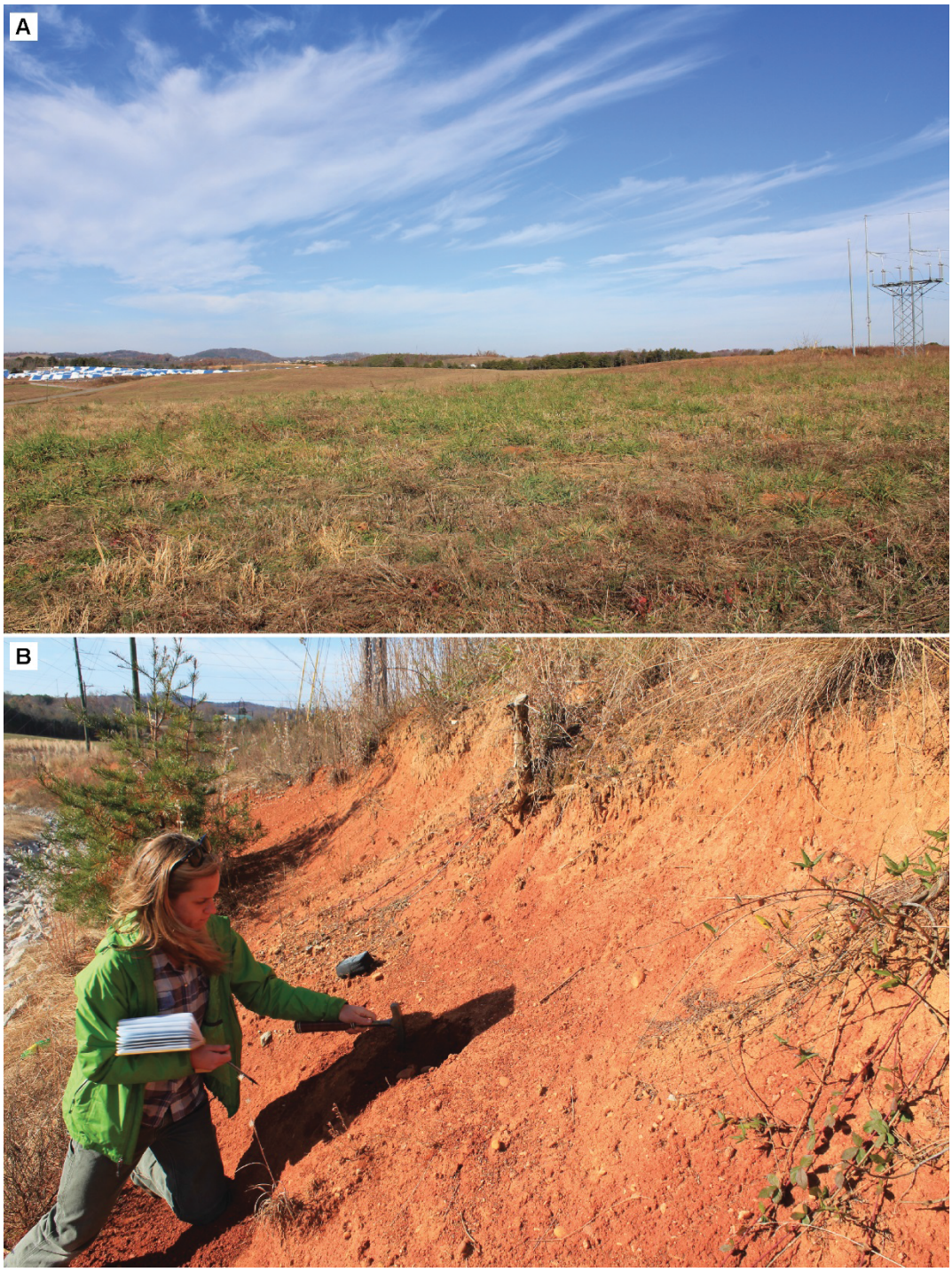

Notes: Photographs taken at Waypoint 240. Photograph A looking west from T9 terrace tread overlooking T7 tread (blue and white buildings). Photograph B showing weathered, rounded gravel deposits in T9 terrace deposit exposure.

Figure 2.5.3-22. Fluvial Terrace Surfaces (A) and Deposits (B) of the Little Tennessee River Exposed along Tellico Reservoir

NRC RAI 02.05.01-02 Question

Residual Stresses in Bedrock

SSAR (Rev 0) Section 2.5.1.2.6.7 Residual Stresses in Bedrock and in SSAR section 2.5.1.2.5.2 Other Local Geologic Hazards indicates that the natural state of stress in a rock is caused by three main factors (Reference 2.5.1-270): previous tectonic forces, current tectonic forces, and weight of the rock. The SSAR provides discussion of previous tectonic forces and the weight of the rock. However, this SSAR section does not discuss the third factor, the current tectonic forces in the area, such as the ETSZ or the current (since Miocene) regional uplift in the southern Appalachians. An understanding of rock stress is a fundamental component of compliance with 10 CFR 100.23 (c-d). Consequently, please provide a discussion of current tectonic forces and develop a rationale for how they might affect residual stress in bedrock and the site.

TVA RAI 02.05.01-02 Response

The discussion of current tectonic forces and contemporary stress, presented in SSAR Subsection 2.5.1.1.4.3.1, is being supplemented with additional material from the literature. The additional text provides more detailed discussion regarding contemporary stress data, presents various hypotheses regarding possible driving mechanisms that define the regional stress patterns in the central and eastern U.S, and discusses the contemporary stress field in terms of the proposed recent (Miocene) uplift of the southern Appalachians.

Recent mantle tomography supports subcontinental lithospheric mantle foundering beneath the southern Appalachians, which is proposed to be the driving mechanism for Miocene buoyant uplift of the southern Appalachians (Reference 1). As such, gravitational body forces acting on the uplifted lithospheric column predictably would generate local horizontal tensile stresses, which in turn could contribute to the subvertical orientation of the intermediate principle stress axis (σ_2) in the southern Appalachians, particularly eastern Tennessee. If ridge-push were the sole driving mechanism that defines the stress field, the intermediate principle axis would not be predicted to be vertical. Therefore, the combination of locally derived upper mantle buoyancy forces and far-field ridge-push forces from the Mid-Atlantic Ridge presents a viable explanation for the observed orientation of regional stresses in the southeastern U.S.

In addition to the discussion above, specific paragraphs within SSAR Subsections 2.5.1.2.5.2 and 2.5.1.2.6.7 are being updated with additional text for clarity. As outlined in SSAR Subsection 2.5.1.2.6.7, residual stresses are not expected in the rock mass at shallow depths at the CRN Site and are not considered to be a hazard during construction or for bearing capacity of the foundation rock mass.

The SSAR changes described above are provided in the following SSAR markups. The SSAR markups will be incorporated in a future revision of the early site permit application.

Enclosure 2
Response to NRC RAI Number 5, Question 02.05.01-02

Reference:

1. Biryol, C.B., Wagner, L.S., Fischer, K.M., and Hawman, R.B., Relationship between observed upper mantle structures and recent tectonic activity across the Southeastern United States: Journal of Geophysical Research, v. 121, p. 3393-4414, 2016.

Enclosure 2
Response to NRC RAI Number 5, Question 02.05.01-02

SSAR Markups

SSAR Subsection 2.5.1.1.4.3.1 is being revised as indicated. Underlines indicates text to be added. Strikethroughs indicates text to be deleted.

2.5.1.1.4.3.1 Current Stress Regime in the Eastern United States

Maps of present day lithospheric stresses provide a wealth of information regarding intraplate seismicity in the eastern United States (e.g., References 2.5.1-181, 2.5.1-182, 2.5.1-183, 2.5.1-184, ~~and~~ 2.5.1-185, and 2.5.1-306) (Figure 2.5.1-21). Orientation of principal stress directions is derived from measurement of instantaneous strain data gathered from hydraulic fracturing, ~~and~~ borehole breakouts, and earthquake focal mechanisms., ~~and indicates the current stress field in the CRN Site 200-mi radius is oriented with maximum horizontal compressive stress trending N45° to N70°E (Reference 2.5.1-183 and 2.5.1-186) (Figure 2.5.1-21). This orientation is consistent with a seismically determined estimate of approximately N55°E, based on focal mechanisms from the Eastern Tennessee Seismic Zone (ETSZ) (Reference 2.5.1-185).~~ The stress field in the Central and Eastern United States (CEUS) and southeastern Canada is broad and consistent on the lateral scale of hundreds of kilometers and is generally characterized by a horizontal, compressive, NE–SW trending maximum horizontal stress (Reference 2.5.1-306). Some second-order stress fields that may deviate from the large-scale regional field and that are driven by more localized forces are also observed across the CEUS (Reference 2.5.1-306).

Compilations of stress indicator data published since the 1980s consistently indicate that the maximum compressive principal stress (σ_1) is subhorizontal, and roughly trends NE-SW across large areas of the CEUS (e.g., References 2.5.1-181, 2.5.1-184, 2.5.1-185, and 2.5.1-306) (Figure 2.5.1-21). A domain of relatively uniform NE-SW-trending σ_1, which includes the northern Atlantic states and parts of southern Canada, was defined by Zoback and Zoback (Reference 2.5.1-307) as the mid-plate stress province. A visual average of long-wavelength σ_1 trends in the mid-plate stress province from maps of stress indicators published by Zoback and Zoback (Reference 2.5.1-181) and Heidbach et al. (Reference 2.5.1-184) is about N55°E to N65°E. The uniformity of the NE-SW σ_1 orientation in the mid-plate stress province is statistically robust (Reference 2.5.1-308) and is generally assumed to extend to the southeastern U.S., with the caveat that stress indicator data are relatively sparse in Georgia, Alabama, and Mississippi, and in neighboring areas of South Carolina and Louisiana.

Although the orientation of σ_1 is relatively uniform throughout the mid-plate stress province (subhorizontal, trending roughly NE-SW), the orientations of the intermediate and minimum compressive stresses (σ_2 and σ_3, respectively) are not. In general, σ_3 is the vertical principal axis (thrust faulting) in the central and northern Appalachians, whereas σ_2 is vertical (strike-slip faulting) in the southern Appalachians and Midwestern Plains states (Figure 2.5.1-21, Sheet 2 of 2). A discussion of the possible driving mechanisms that result in the observed regional stress field is presented later in this subsection.

Mazzotti and Townend (Reference 2.5.1-185) define the orientation and shape of the stress ellipsoid (orientation and magnitude of the three principal stress axes) throughout the eastern U.S. by inverting groups of small-earthquake focal mechanisms. Their analysis focuses on areas of relatively higher background seismicity rates, where a sufficient number of focal mechanisms are available to provide an over-determined inversion solution. Areas of elevated seismicity rate closest to the CRN Site include: (1) the Eastern Tennessee seismic zone; (2);

the epicentral region of the 1886 Charleston, South Carolina earthquake; and (3) the New Madrid seismic zone region (Figure 2.5.1-21). The inversion results for these regions indicate that σ_1 is subhorizontal and oriented NE-SW to ENE-WSW, consistent with the regional trend in the mid-plate stress province. σ_3 is vertical in the region surrounding Charleston (Reference 2.5.1-309), whereas the New Madrid and the Eastern Tennessee seismic zones are characterized by vertical σ_2 axes, which are more indicative of strike-slip faulting. Chapman et al. (Reference 2.5.1-194) and Cooley (Reference 2.5.1-310) also present focal mechanisms from the Eastern Tennessee seismic zone that indicate σ_2 locally is vertical and the style of deformation is characterized by strike-slip faulting.

Hurd and Zoback (Reference 2.5.1-306) use the inversion results of Mazzotti and Townend (Reference 2.5.1-185), with an updated catalog of available earthquake focal mechanisms, to produce a map of the regional variation stress-field geometry (Figure 2.5.1-21, Sheet 2 of 2). They report a strike-slip focal mechanism from a M_w 3.8 earthquake that occurred in 2009 in central Alabama approximately 350 km south of the CRN Site, which indicated left-lateral slip on a sub-vertical, WNW-ESE-striking nodal plane (alternatively, right-lateral slip on a NNE-SSW plane). T he P-axis for this focal mechanism trends approximately N50°E, which is consistent with the inferred regional NE-SW trend of σ_1 in the mid-plate stress province, and the inferred strike-slip kinematics suggest that σ_2 is vertical and σ_3 is horizontal in the vicinity of the earthquake.

Potential Driving Mechanism of Stresses in the Eastern United States

Zoback and Zoback (Reference 2.5.1-307) note that the consistent NE-SW orientation of σ_1 across very large areas of the interior of the North American plate implies relatively uniform forces acting on its boundaries, and proposed that the dominant source of stress for the mid-plate stress province is ridge-push force from the Mid-Atlantic Ridge. Richardson and Reding (Reference 2.5.1-311) modeled the contributions of several classes of forces to the state of stress in the interior of North America:

- Horizontal stresses arise from gravitational body forces acting on lateral variations in lithospheric density. Richardson and Reding (Reference 2.5.1-311) emphasize what is commonly called the ridge-push force is an example of this class of force. Rather than a line force that acts outwardly from the axis of a spreading ridge, ridge-push arises from the pressure that the positively buoyant, topographically high ridge exerts against the topographically lower and less buoyant lithosphere in the adjacent ocean basins. The horizontal pressure from the ridge results in large compressive stresses in the oceanic lithosphere, which are transmitted elastically into the interior of adjoining continents.
- Shear and compressive stresses are associated with major tectonic plate boundaries like transform faults and subduction zones.
- Shear tractions act on the base of the lithosphere from relative flow of the underlying asthenospheric mantle.

Richardson and Reding (Reference 2.5.1-311) conclude that the NE-SW trend of σ_1 in the central and eastern U.S. dominantly reflects the contribution from ridge-push forces. They estimate the magnitude of ridge-push to be about 2 to 3 x 10^{12} N/m (i.e., the total vertically integrated force acting on a column of lithosphere 1 m wide), which corresponds to average stresses of about 40 MPa to 60 MPa in a 50-km-thick elastic plate. Richardson and Reding (Reference 2.5.1-311) demonstrate that the fit of modeled stress trajectories to the data is

improved by adding a modest compressive stress (about 5 to 10 MPa) acting on the San Andreas fault and Caribbean plate boundaries.

The observed NE-SW orientation of σ_1 in the mid-plate stress province is reproduced by models that assume relative flow of the underlying asthenosphere induces a shear stress (i.e., "drag") on the base of the continental lithosphere (Reference 2.5.1-311). However, Richardson and Reding (Reference 2.5.1-311) and Zoback and Zoback (Reference 2.5.1-307) discount this as a significant contribution to the total stress in the continental interior, because it predicts that the horizontal compressive stress should increase by an order of magnitude, from east to west, across the central U.S. This east-to-west stress increase is not observed. In fact, Hurd and Zoback (Reference 2.5.1-306) demonstrate the magnitude of σ_1, relative to σ_2 and σ_3, is higher in the northeastern U.S. than in the southeastern and central U.S., which essentially contradicts the first-order predictions of the "drag" model. More recent research (Reference 2.5.1-312) suggests there may be a partially molten, low viscosity channel at the base of the lithosphere that mechanically decouples the tectonic plates from the asthenosphere. If this model is valid, then it is unlikely that significant shear stresses in the lithosphere, specifically in the upper crust, are a product of motion relative to the asthenosphere.

Additionally, the orientation of the principal stress axes in the southern Appalachians (specifically, σ_2 vertical) is inconsistent with ridge push as the lone driving mechanism for the observed stress field. If ridge push were the sole driving mechanism, then σ_3 should be vertical with nearly horizontal σ_1 and σ_2, similar to what is observed in the central and northern Appalachians (Figure 2.5.1-21, Sheet 2 of 2). While the orientation of σ_1 is consistent with the predicted orientation based on the orientation of the mid-Atlantic Ridge (Reference 2.5.1-307), a subvertical intermediate principal stress axis suggests local buoyancy forces in the southern Appalachians may be contributing to the overall shape and orientation of the regional stress field. Numerous independent studies in recent decades have interpreted Cenozoic epeirogenic uplift of the Southern Appalachians (see Subsection 2.5.1.1.2), and many workers attribute the uplift to mantle processes. Based on recently acquired mantle tomography, Biryol et al. (Reference 2.5.1-313) suggest that foundering of the lower lithosphere beneath west-central Tennessee is driving buoyant uplift of eastern Tennessee, Georgia, and South Carolina (Figure 2.5.1-82). Gravitational body forces acting on the uplifted lithospheric column predictably would generate local horizontal tensile stresses, which in turn could contribute to the subvertical orientation of σ_2 in the southern Appalachians (see discussion and additional references cited in Reference 2.5.1-314). The combination of locally derived upper mantle buoyancy forces and far-field ridge-push forces from the Mid-Atlantic Ridge presents a viable explanation for the observed orientation of the regional stress field in the southeastern U.S. including the site region.

Enclosure 2
Response to NRC RAI Number 5, Question 02.05.01-02

The second paragraph of SSAR Subsection 2.5.1.2.5.2 is being revised as indicated. Underlines indicates text to be added. Strikethroughs indicates text to be deleted.

2.5.1.2.5.2 Other Local Geologic Hazards

Paragraph 2

The potential for unrelieved residual stresses in the bedrock or soil can be evaluated from an understanding of the geologic history of the Clinch River area. As described in Subsection 2.5.1.2.4, ~~T~~the CRN Site last experienced major tectonic uplift in the Pennsylvanian and Permian periods during the Alleghanian orogeny, which caused the folding and faulting observed today. At this time the Paleozoic strata on which the site is located were uplifted and gently folded. As described in Subsection 2.5.1.1.4.3.1, the CRN Site is located in the Eastern U.S. stress regime, which is characterized as a broad and consistent stress field. The history of the CRN ~~site~~ Site since the Alleghanian orogeny has been one of steady weathering and erosion.

The third and fifth paragraphs of SSAR Subsection 2.5.1.2.6.7 are being revised as indicated. Underlines indicates text to be added. Strikethroughs indicates text to be deleted.

2.5.1.2.6.7 Residual Stresses in Bedrock

Third paragraph:

High residual stress is not expected in the rock mass at the CRN Site. As described in Subsection 2.5.1.2.4, bedrock at the site has been subject to previous tectonic stresses as characterized by the parallel valleys and ridges formed by differential erosion of folded and faulted Paleozoic age sedimentary strata. The deformational event responsible for the development of this Appalachian fold-thrust belt is the Alleghanian orogeny that occurred during the late Paleozoic Era. Since this time, the bedrock has undergone gradual relaxation through weathering and erosion and there is no evidence to suggest recent (during the Quaternary Period) tectonic activity has occurred at the site (see Subsections 2.5.1.2.2, 2.5.1.2.4, and 2.5.3.2). Unlike much of the northeastern United States, the southeastern United States including Tennessee has not been subject to stresses induced through glacial loading. Stress-relief features such as those described above have not been observed or reported at the CRN Site.

Fifth paragraph:

Current tectonic forces in the site region and the associated broad stress regime of the Eastern U.S. (see Subsection 2.5.1.1.4.3.1) as well as any ~~High~~ residual stresses, are not expected in the rock mass at shallow depths (hundreds of feet) at the CRN Site and are not considered to be a hazard during construction or for bearing capacity of the foundation rock mass.

Enclosure 2
Response to NRC RAI Number 5, Question 02.05.01-02

The following references are being added to SSAR Subsection 2.5.1.3. Underlines indicates text to be added.

2.5.1.3 References

2.5.1-306. Hurd, O., and Zoback, M.D., Intraplate earthquakes, regional stress and fault mechanics in the Central and Eastern U.S. and Southeastern Canada: Tectonophysics, v. 581, p. 182-192, 2012.

2.5.1-307. Zoback, M.L., and Zoback, M.D., Tectonic stress field of the continental United States, in Pakiser, L.C., and Mooney, W.D., Geophysical framework of the continental United States: Geological Society of America Memoir 172, 1989.

2.5.1-308. Coblentz, D.D., and Richardson, R.M., Statistical trends in the intraplate stress field: Journal of Geophysical Research, v. 100, no. B10, p. 20245-20255, 1995.

2.5.1-309. Chapman, M.C., Beale, J.N., Hardy, A.C., and Wu, Q., Modern seismicity and the fault responsible for the 1886 Charleston, South Carolina, earthquake: Bulletin of the Seismological Society of America, v. 106, no. 2, p. 364-372, 2016.

2.5.1-310. Cooley, M.T., A new set of focal mechanisms and a geodynamic model for the Eastern Tennessee Seismic Zone [M.S. thesis]: Memphis, University of Memphis, 46 p, 2014.

2.5.1-311. Richardson, R.M., and Reding, L.M., North American plate dynamics: Journal of Geophysical Research, v. 96, p. 12201-12223, 1991.

2.5.1-312. Stern, T.A., Henrys, S.A., Okaya, D., Louie, J.N., Savage, M.K., Lamb, S., Sato, H., Sutherland, R., and Iwasaki, T., A seismic reflection image for the base of a tectonic plate: Nature, v. 518, p. 85-88, 2015.

2.5.1-313. Biryol, C.B., Wagner, L.S., Fischer, K.M., and Hawman, R.B., Relationship between observed upper mantle structures and recent tectonic activity across the Southeastern United States: Journal of Geophysical Research, v. 121, p. 3393-4414, 2016.

2.5.1-314. Molnar, P., and Lyon-Caen, H., Some simple physical aspects of the support, structure, and evolution of mountain belts, in Clark, S.P. Jr., Burchfiel, B.C., and Suppe, J., eds., Processes in Continental Lithospheric Deformation: Geological Society of America Special Paper 218, p. 179-207, 1988.

Enclosure 2
Response to NRC RAI Number 5, Question 02.05.01-02

A second sheet, Sheet 2, is being added to existing SSAR Figure 2.5.1-21. The title of Figure 2.5.1-21 (Sheet 1) is updated accordingly:

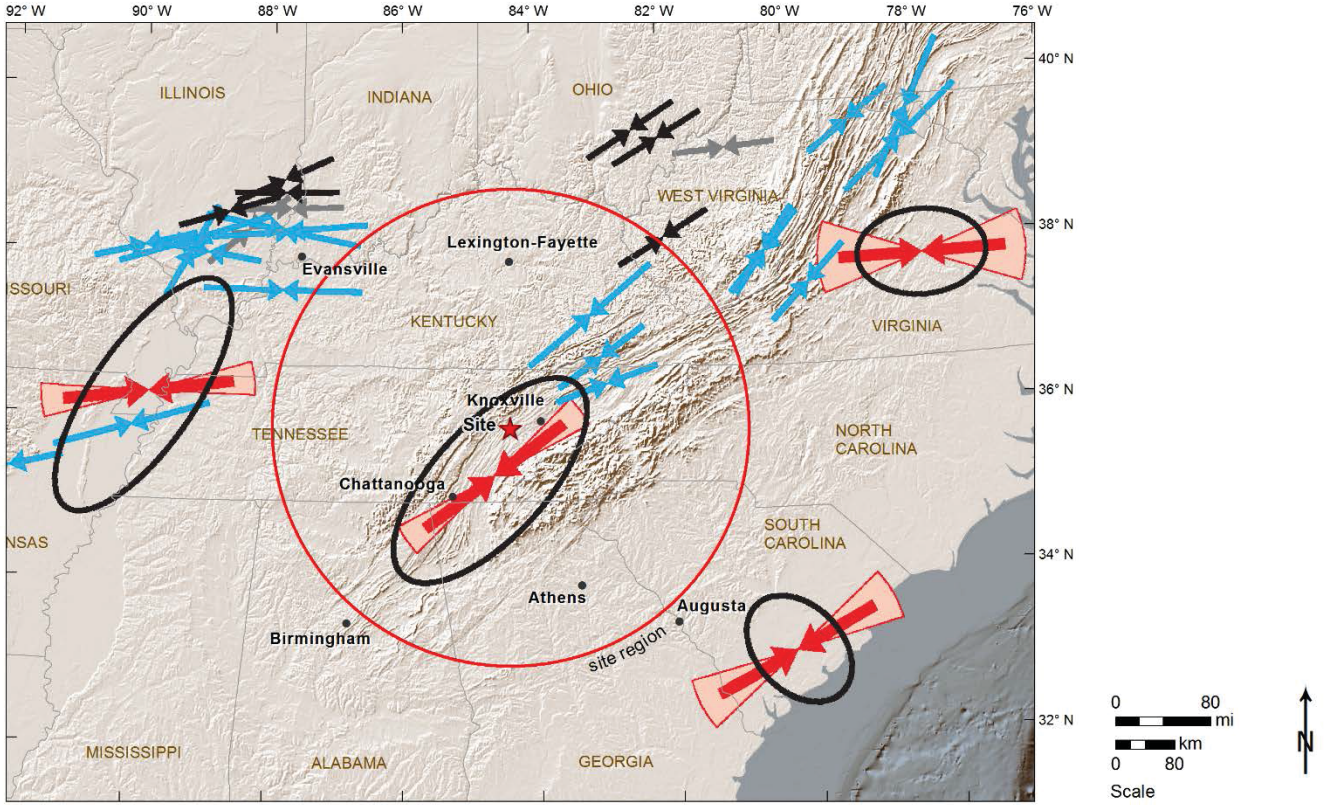

Notes:
Map of current stresses in the central and eastern U.S. (after Reference 2.5.1-185).
Black and gray arrows – orientation from borehole observations;
Blue arrows – borehole observations used in calculating the regional average within 250 km (155 mi) of the seismic zones (solid ellipses);
Red arrows and angular sectors – orientation from focal mechanism inversion.

Figure 2.5.1-21. (Sheet 1 of 2) Current Compressive Stress—Eastern United States

Enclosure 2
Response to NRC RAI Number 5, Question 02.05.01-02

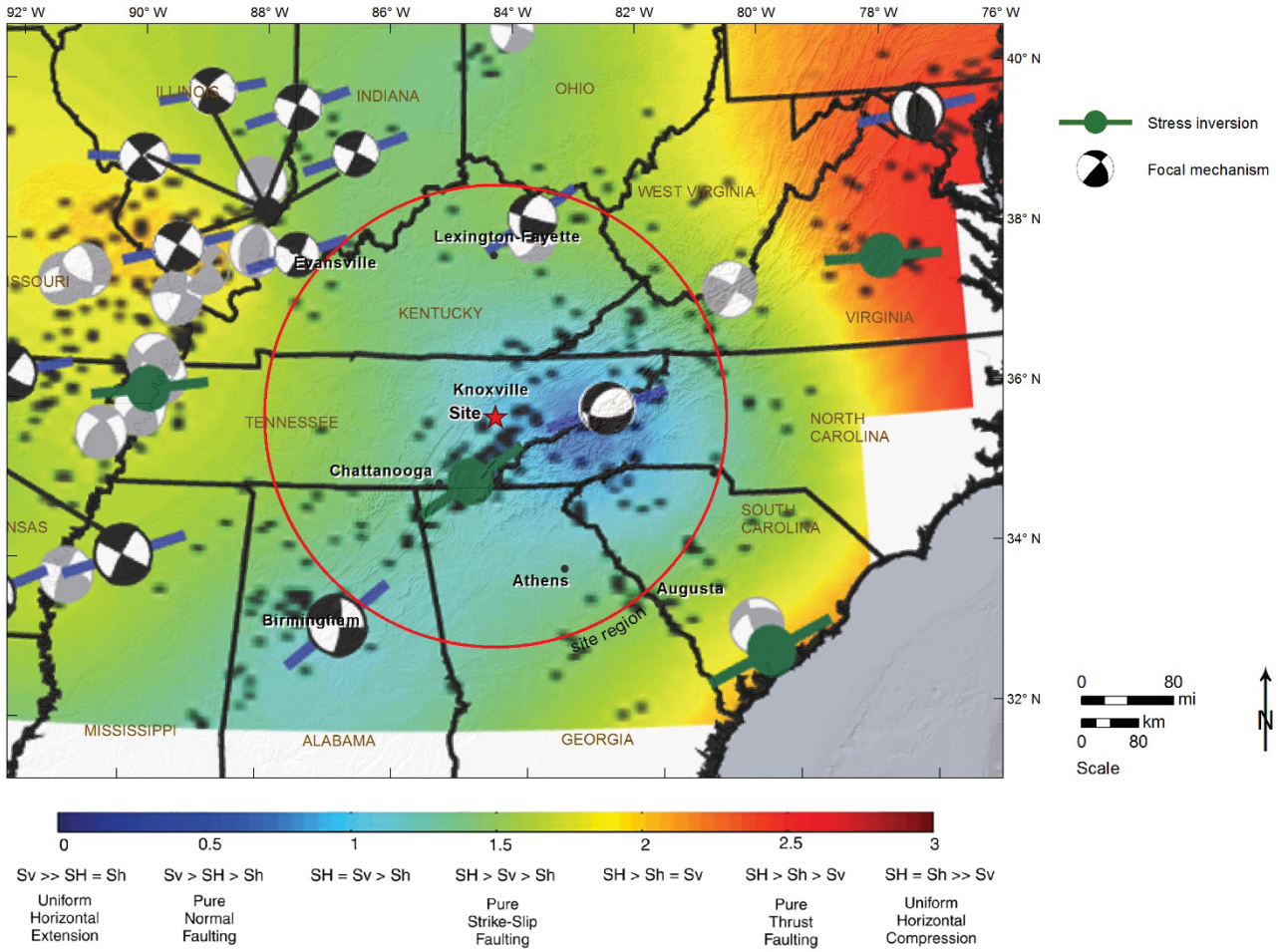

Notes:
Gray focal mechanisms from Reference 2.5.1-183; black focal mechanisms from Reference 2.5.1-306.
SH – maximum horizontal stress; Sh – minimum horizontal stress; Sv – vertical stress.

Source: Reference 2.5.1-306

Figure 2.5.1-21. (Sheet 2 of 2) Regional Stress Map from Hurd and Zoback

New Figure 2.5.1-82 is being added to SSAR Subsection 2.5.1:

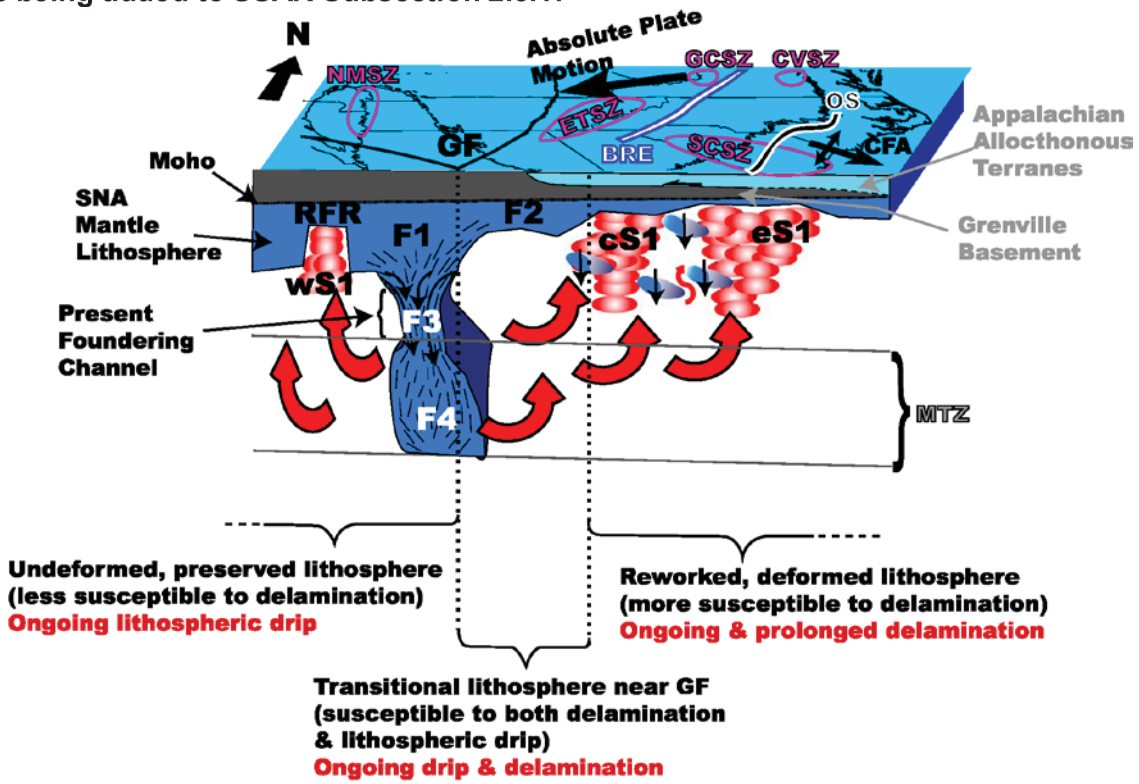

Notes:
BRE – Blue Ridge escarpment; CFA – Cape Fear arch; GF – Grenville front; OS – Orangeburg scarp; RFR – Reelfoot rift; CVSZ – Central Virginia seismic zone; ETSZ – East Tennessee seismic zone; GCSZ – Giles County seismic zone; SCSZ – South Carolina seismic zone; NMSZ – New Madrid seismic zone; SNA – Stable North America.
F1, F2, F3, F4, cS1, eS1, and wS1 correspond to geophysical anomalies.

Source: Reference 2.5.1-313

Figure 2.5.1-82. Conceptual Model of Upper Mantle Structure Beneath the Southeastern U.S.

Enclosure 3

Response to NRC RAI Number 6, Question 02.05.04-01

NRC RAI 02.05.04-01

Rock mass properties determination

In SSAR (Rev 0) Section 2.5.4.2.4.4, it states that the rock mass properties are developed using the Geological Strength Index (GSI) classifications of the stratigraphic units. The site investigation data indicates the presence of rock discontinuities and fractures in the stratigraphic units, and the weathered or fracture zones typically occur along bedding planes at the CRN sites (SSAR 2.5.1.2.6.3 "Fracture Zones"). The rock mass discontinuities and fracture zones may result in pre-determined shear failure surfaces. Because the GSI chart may not be applicable when structural planes of the rock control the failure of rock mass [Ref.1], and the rock mass property is a key input for the evaluations of foundation stability, please discuss how the inclined rock formation interfaces were taken into account when determining the rock mass properties to ensure the proper evaluations of subsurface material and foundation stability to meet the requirements of 10 CFR 100.23 (d)(4).

Reference 1: Hoek, E. and Marinos, P. (2000): Predicting Tunnel Squeezing. Tunnels and Tunnelling International. Part 1 – November 2000, Part 2 – December, 2000.

TVA RAI-02.05.04-01 Response

The use of the GSI classification system to develop rock mass properties of the inclined rock units at the CRN Site is supported by discrete inspection of rock core, interpretation of downhole geophysical survey data, and observations during field mapping. Both visual inspection of rock core and interpretation of downhole geophysical data were used to characterize the discontinuities in the rock units. These characterizations are presented in SSAR Subsection 2.5.1.2.6 and are discussed below. A grouting program was conducted during the Clinch River Breeder Reactor Project (CRBRP) investigation. Observations from this program, as noted below, are also used to characterize the rock units at the CRN Site. In addition, observations reported during CRBRP construction, the excavation specifically, are discussed below and are used to support site characterization. Results from these various data sets corroborate the characterization of the rock mass discontinuities and fracture zones of the inclined rock units and validate the use of the GSI classification system for the evaluation of foundation stability.

Note that a finite element model using PLAXIS 2D analysis software (References 1 and 2) considers alternative characterizations of weathering, discontinuities, and fracture zones. Results from this model are presented in SSAR Subsection 2.5.4.13.

Terminology used in this response include the following:

- Contact – "boundary between two units that is identified on the basis of a compositional, textural, structural, or temporal difference between the units" (Reference 3), such as a geologic formation contact or geologic member contact, e.g., Benbolt-Rockdell contact.
- Fracture – a break in the rock, and may include mechanical fractures in rock cores and healed (naturally cemented) fractures.

- Fracture zone – a zone of closely-spaced breaks in the rock, and may include mechanical fracture zones in rock cores, and healed natural fracture zones.
- Shear-fracture zone – at the CRN Site, this consists of calcite-healed fracture zone containing slickensides that are indicative of previous rock shearing or interbed slippage (SSAR Subsection 2.5.1.2.4.3.4).
- Discontinuity – a natural unhealed fracture in the rock, includes bedding joints and other joint types, as well as faults, but excludes mechanical breaks in rock core, healed fractures or healed joints, and healed faults.
- Bedding plane – planar surface between sedimentary beds, e.g., contact between siltstone and limestone beds of uniform thickness, and may or may not include fractures or joints.
- Bedding structure – includes planar bedding, irregular bedding, discontinuous bedding, and anastomosing bedding (Reference 4, Appendix C).
- Joint – a natural (*in situ*) rock fracture associated with a dominant orientation, includes joints along bedding and joint sets with other orientations (excludes mechanical fractures and healed fractures).
- Joint set – a set of natural fractures with similar orientation, i.e., similar strike and dip.
- Interface – elements used in numerical models to form a boundary between materials having different properties.
- Inclined rock formation interface – interface elements used to model discontinuities and contacts in finite element (FE) modeling along inclined bedding, with reduced strength resulting from assumed weathering or higher degree of fracturing compared to adjoining rock mass.

Applicability of GSI to Rock Mass Strength Estimates

Reference 5 provides an updated version of the GSI chart, shown in SSAR Figure 2.5.1-58, that allows quantification of GSI from rock cores by using the Rock Quality Designation (RQD) and the Joint Condition rating parameter, $JCond_{89}$. Reference 6 provides a version of GSI that specifically is developed for flysch (i.e., weak heterogeneous rock mass, which is different than the strong jointed rock mass at the CRN Site). Figure 4 from Reference 5 indicates that GSI is applicable to rock masses with many joint sets that create interlocking blocks of rock and where the block sizes are small relative to the length of the potential failure surface. SSAR Subsection 2.5.1.2.4.3.3 discusses four joint sets identified for the CRBRP and five joint sets identified for the CRN Site. The presence of multiple joint sets makes the GSI applicable to the rock mass.

SSAR Subsection 2.5.4.2.4.4 discusses the use of GSI in the Hoek-Brown nonlinear rock mass failure criterion to estimate rock mass strength (Reference 7). The applicability of GSI and the Hoek-Brown failure criterion to a rock mass, however, does not preclude using other failure criteria to assess alternative modes of failure for the same excavation. Jointed rock masses may have more than one potential mode of failure for rock cuts, including planar, wedge, and toppling failures. An example of an alternative rock strength model is the Barton-Bandis nonlinear joint failure criterion for planar shearing failure, but this requires a continuous rock discontinuity to be present (Reference 8). The following text discusses why a predetermined continuous planar surface below the power block area is not likely.

Enclosure 3
Response to NRC RAI Number 6, Question 02.05.04-01

Rock Mass Discontinuities and Fracture Zones

Site information regarding rock mass discontinuities and fracture zones is available in the following sources:

- Geotechnical coring logs and rock core photographs, with detailed descriptions of discontinuity conditions and weathering (Reference 4);
- Acoustic televiewer logs, with frequency, orientation, and other characteristics of rock structure and discontinuities (Reference 4); and
- Shear fracture zones, as discussed in SSAR Subsections 2.5.1.2.4.3.4 and 2.5.1.2.6.4.

Geotechnical Coring Logs and Rock Core Photographs

Weathered or fracture zones typically occur along bedding planes and typically occur within weathered rock in the uppermost 100 ft. Below this weathered zone, rock mass discontinuities typically are tighter, less frequent, and less persistent (shorter), and this fact will be clarified in the SSAR by adding text to Subsections 2.5.1.2.6.3, 2.5.4.2.4.4, and 2.5.4.10.1.2. Weathered or fracture zones are discussed in SSAR Subsection 2.5.1.2.6.3, Fracture Zones. The following observations are based on geotechnical coring logs, rock core examination and photographs:

- These zones typically represent fair to poor quality rock, consisting of multiple, open to healed, slightly to highly weathered joints or bedding planes, some calcite-filled, with occasional core loss and loss of drilling fluid.
- A summary of weathered or fracture zones (greater than 0.9 ft thick [apparent thickness along boring axis]) encountered in the 100- and 200-series borings drilled at the CRN Site is contained in SSAR Table 2.5.1-16 and shown on SSAR Figure 2.5.1-59.
- The majority of the fracture zones are encountered between elevations of approximately 800 and 750 ft NAVD88.

Reference 4, Table B.1.1, explains the fracture description codes. SSAR Table 2.5.1-16 lists 52 fracture zones, with ten of those zones occurring below the power block area, at about elevation 683 ft NAVD88. Table 1 (below) provides descriptions of the ten zones below the power block. Four zones that include bedding joints (BJs) are highlighted in bold font in Table 1.

Enclosure 3
Response to NRC RAI Number 6, Question 02.05.04-01

Table 1 – Fracture Zones Below Power Block

Boring	Elevation, ft NAVD88	Depth, ft	Descriptions
MP-101	666.2 - 664.2	134.3 - 136.3	FZ, 60°, PR, VT, A, I, with calcite
MP-109	642.0 - 640.9	157.9 - 159.0	FZ, 80-90°, SR, VT, A, I, with calcite
MP-120	570.1 - 568.2	230.0 - 231.9	**FZ (8 BJs) 30°, US, T, B, II; FZ (6 BJs), 30°, US, T, B, II**
MP-201	553.2 - 551.2	237.7 - 239.7	**FZ (10 BJs), 20-30°, PR-UR, T-PO, A-B, I-II; FZ (5 BJs), 30°, PR, T-PO, B-C, II**
MP-201	497.2 - 491.0	293.7 - 299.9	**FZ (7 BJs), 30°, PR-SR, A-C, I-II; FZ (8 BJs), 30°, PR, T-PO, B, II** / J, 60°, PR, O, B, II; 0.3' loss of core; FZ, 30°, PR, PO-O, D-K, II-IV; FZ, 20-40°, PR, PO, C-G, II-III; FZ, 30°, PR, PO-O, II-IV; mechanically broken rock with loss of recovery
MP-201	390.3 - 387.7	400.6 - 403.2	FZ, 20-80°, VT, A, I, intact, healed with dolomite and trace indurated siltstone/clay; FZ, 0-20°, PR, O, B, I, 0.3' loss of core (mechanically broken)
MP-202	532.7 - 531.7	279.1 - 280.1	**FZ, BJ (6), 30°**, and J, 0°
MP-203	660.7 - 659.2	130.8 - 132.3	FZ, 30°, PR-PS, O, B, II
MP-205	629.4 - 627.5	181.5 - 183.4	FZ, core loss of 1.3'
MP-209	609.2 - 608.2	198.5 - 199.5	FZ, 60°, SR, O, C, III, core loss (mechanical) from 199.2 to 199.5'

Bedding joints typically are not weathered or weakened below the power block elevation, as indicated by an aperture rating of VT to T (very tight to tight), fracture filling rating of A or B (tightly healed to unaltered joint walls), and seepage rating of I to II (very tight or dry). Fracture filling rating of C (slightly altered joint walls or clay-free mineral coatings, e.g., calcite), and seepage rating of III (dry but evidence of water flow, i.e., iron oxide staining) is indicative of slight surficial weathering but not significant weakening, i.e., not sufficient to significantly affect foundation stability.

From all the 100-series and 200-series borings, SSAR Table 2.5.1-16 includes only one zone (MP-201, depth 293.7-299.9 ft) with both bedding joints and notable weathering or weakening within the fracture zone. That zone includes aperture ratings of PO to O (partially open to open) and fracture filling ratings of D to K (non-softening clay coatings to zones/bands of crushed rock and continuous non-softening over-consolidated clay less than 5 mm thickness).

The above discussion indicates that weathered and fracture zones below the power block foundation are limited in extent and not likely to result in a predetermined weathered and weakened planar failure surface.

In addition to the weathered and fracture zones summarized in SSAR Table 2.5.1-16 and discussed above, the conditions of individual bedding joints were assessed for weathering and/or weakening, based on the geotechnical coring logs and rock core photographs. Several 100-series, 200-series and 400-series borings were selected for this assessment, based on those with acoustic televiewer data that are representative of the geologic formations and foundation locations at the CRN Site. The result of this assessment is that about 3 percent of the bedding joints indicate significant weathering or weakening below a depth of 100 ft. Additional details of this assessment are provided below.

From an assessment of rock core logs and photographs from 15 borings (MP-101, MP-102, MP-111, MP-112, MP-113, MP-120, MP-201, MP-202, MP-212, MP-213, MP-219A, MP-412, MP-416, MP-421 and MP-424), the following conditions are indicated for bedding fractures and joints in core runs with drilled depths greater than about 60 ft:

- A total of 2871 fractures and joints.

- A total of 1997 bedding joints and associated fracture zones, ranging in depth from 60.4 ft to 537.8 ft.
- A total of 1912 bedding joints and fracture zones have fracture infilling ratings of A (tightly healed), B (unaltered), or C (slightly altered or clay-free mineral coatings, e.g., calcite), and seepage rating of I (very tight and dry), II (dry with no evidence of water flow), or III (dry but evidence of water flow, i.e., iron oxide staining).

For bedding joints at drilled depths greater than about 100 ft:

- A total of 57 bedding joints and associated fracture zones have fracture infilling ratings of D to H (non-softening clay coatings to softening clay fillings less than 5 mm thickness), or have seepage rating of IV (damp but no free water present). This number is 2.9 percent of the total number of 1997 bedding joints and fracture zones.
- A total of 8 bedding joints have fracture infilling ratings of F to H (thin mineral filling). This number is 0.4 percent of the total number of bedding joints.
- Only 1 bedding joint has fracture infilling rating greater than F (i.e., rating of H, with softening clay filling less than 5 mm thickness).

Based upon the summary of site fractures above, the infrequent occurrences (about 3 percent) of notable weathering along bedding joints below a drilled depth of 100 ft are not within one particular zone, are absent in some boreholes, and apparently are at random locations and depths within the various formations at the CRN Site. This information indicates that bedding joints are not likely to result in a continuous predetermined weakened planar failure surface below the power block foundation level. This conclusion is being clarified in the SSAR with addition of text to Subsections 2.5.4.2.4.4 and 2.5.4.10.1.2.

Acoustic Televiewer Logs

In addition to the geotechnical coring logs and rock core photographs discussed above, the conditions of individual discontinuities identified in the acoustic televiewer (ATV) logs were assessed for weathering and/or weakening. All of the 100-series and 200-series borings with ATV logs in Reference 4 (Appendix C) are included in this assessment. A few of the 400-series borings also are included to provide a more complete representation of the geologic formations at the CRN Site. The result of this assessment is that 1.7 percent of all joints are parallel to bedding planes, open, and occur below a drilled depth of 100 ft, indicating weathering or weakening at the foundation level is infrequent and likely not continuous along bedding planes. Additional details of this assessment are provided below.

From an assessment of acoustic televiewer data from 14 borings (MP-101, MP-102, MP-111, MP-112, MP-113, MP-120, MP-201, MP-202, MP-212, MP-213, MP-219A, MP-412, MP-416 and MP-421) (Reference 4), the following conditions are identified for all fractures (bedding parallel and other orientations) and bedding structures (not fractures):

- A total of 2438 bedding structures, ranging in drilled depth from 8.4 ft to 537.1 ft.
- A total of 860 fractures, ranging in drilled depth from 6.2 ft to 536.4 ft.
- A total of 84 open fractures, ranging in drilled depth from 6.2 ft to 366.1 ft, and are characterized as either discontinuous, irregular or planar open fractures. This number is about 10 percent of the total fractures.

For fractures at drilled depths greater than about 100 ft:

- A total of 18 fractures are identified as open and planar. This number is 2.1 percent of the total number of 860 fractures.
- A total of 15 fractures are identified as open, planar, and have orientations similar to the average bedding orientation, i.e., moderate dip to the southeast. This number is 1.7 percent of the total number of fractures.

The infrequent occurrence (less than 2 percent) of notable weathering along bedding joints below a drilled depth of 100 ft are not within one particular zone, are absent in some boreholes, and apparently are at random locations and depths within the various formations at the CRN Site. This information indicates that bedding joints are not likely to result in a continuous predetermined weakened planar failure surface below the power block foundation level. This conclusion is being clarified in the SSAR with the addition of text to Subsections 2.5.4.2.4.4 and 2.5.4.10.1.2.

Shear-Fracture Zones

Shear-fracture zones are parallel to sub-parallel to bedding, but importantly are healed by calcite infilling and therefore are not planes of weakness. This characteristic of having been healed is discussed in SSAR Subsections 2.5.1.2.4.3.4 and 2.5.1.2.6.4 as follows, with underlining added to indicate the healed nature of the shear-fracture zones:

- SSAR Subsection 2.5.1.2.4.3.4 states that “shear-fracture zones consist of intensely fractured, calcite-healed zones that are conformable with bedding.”
- SSAR Subsection 2.5.1.2.6.4 states that “shear-fracture zones are typically zones of multiple, closely spaced, tightly healed, calcite filled shear fractures with occasional, primarily discrete, fracture zones and the fractures commonly form orthogonal to bedding. The quality of the rock within these zones is generally high, unless associated with fracture zones.”
- SSAR Subsection 2.5.1.2.6.4 also states that the shear zone encountered in the lower portion of the Eidson Member “is described as a hard, re-healed, cemented zone.”
- SSAR Subsection 2.5.4.1.3.2 also states that “descriptions of the borings indicate that the shear-fracture zones are typically zones of multiple, closely spaced, tightly healed, calcite filled shear fractures.”
- SSAR Figure 2.5.1-68 is schematic diagram of a shear-fracture zone with “slickensided, calcite-healed shear fracture surfaces”.

CRBRP Observations from Test Grouting Program

CRBRP observations regarding rock mass discontinuities and fracture zones are available from the test grouting program (References 9 and 10).

Reference 9 (Appendix 2-C, p. 2C-1) summarizes a test grouting program for verifying the homogeneity and the satisfactory bearing quality of the foundation strata. Test grouting was performed within two stratigraphic zones and at 13 locations within an area 40 ft by 40 ft (p. 2C-2, and Figures 2 and 3, in Reference 9):

- Zone III – Elevation 732 MSL to 5 feet above limestone contact, and
- Zone IV – 5 feet above limestone contact to 10 feet below lower siltstone contact.

The siltstone in Zone III and the underlying limestone in Zone IV correspond to the Fleanor Member and the Eidson Member, respectively. Reference 9 (p. 2C-7) concluded the following from the test grouting program: "All of the zones in which test grouting was performed are relatively impenetrable to cement grout. Grout takes were very small, on the order of 0.003 to 0.03 cubic foot per foot of hole at grouting pressures of 30 psi."

The test grouting program also included water pressure testing within three zones at five locations (Tables I and II): Zone II – Top of rock to elevation 732 ft MSL, and Zones III and IV described above. The elevation difference between MSL NGVD29 in Reference 9 and NAVD88 in the SSAR is less than one foot. Reference 9 (p. 2C-7 and Table II) concluded the following from the water pressure testing:

- Changes in water levels resulted while water pressure testing at adjacent holes.
- The apparent connection between holes is attributed to bedding partings and thin joints.
- The ability to maintain the test pressures of 20 to 30 psi indicates that such discontinuities are small.
- Water pressure re-testing at center of test area after grouting indicates that the rock mass hydraulic conductivity was lowered, with much larger reduction in Zone III (90 ft/yr to 2 ft/yr) than Zone IV (50 ft/yr to 14 ft/yr).

The reduced effectiveness of grouting in the deeper Zone IV may be attributed to tighter and less interconnected rock mass discontinuities (bedding separations and other joints).

Reference 10 (Subsection 2.5.1.3, Limestone Solutioning) indicates: “As jointing becomes less frequent and tighter with depth, there is an approximate lower limit to which significant solutioning has occurred. The applicants have identified that level, referred to as the ‘depth to continuous rock,’ and plan to place structural foundations below it at a base level of 712.5 ft MSL.” The NRC Staff cites two site characteristics relevant to weathered or fracture zones along bedding joints in its conclusions regarding absence of significant cavities below the foundations: (1) the tightness and low frequency of joints below top of continuous rock, and (2) a test grouting program which demonstrates by low grout takes that the rock contains few voids. In addition to the staff conclusion that the low grout takes indicate few solutioning voids, the test grouting results also indicate few open fractures. Conclusions from the test grouting program is being added in the SSAR by adding text to Subsection 2.5.4.2.4.4.

CRBRP Observations from Construction Excavation

Additional CRBRP information regarding rock mass discontinuities and fracture zones is available from rock excavation observations, including rock mass descriptions and geological maps (Reference 11).

Excavation for the CRBRP nuclear island (NI) was about 100 ft deep, 480 ft long and 360 ft wide. Observations of the CRBRP NI excavation (Reference 11, p. 3-21) are consistent with CRN Site investigation data regarding the absence of continuous open and/or weathered fractures along bedding planes (or any other joint sets) at foundation level. These observations include:

- Although fracture porosity and corresponding permeability may be high in the weathered zone, they are sharply reduced with depth because these discontinuities become tighter, less frequent, shorter, and with a strongly subdued hydraulic connection.
- For this reason, the NI base at El. 714 ft MSL has hardly exhibited any seepage in spite of the fact that it is far below the groundwater table and about 27 ft below the Clinch River.
- Similarly, the drain pipes installed in the NI walls at a 10-ft spacing are mostly dry, although some are wet due to slight continuous seepage, but none shows real flow. Regardless of a high hydraulic gradient toward the NI excavations, leakage into the excavation is very small and slow.

Additional observations of the CRBRP excavations indicate significant changes with depth in weathering and rock mass discontinuity conditions (Reference 11, p. 3-20):

- There is a relatively sharp boundary between weathered and fresh rocks in the excavations, and it coincides with bedding planes.
- Considering the extent to which rock characteristics change with depth, using such criteria as joint frequency, size of opening, and type of filling in strike joints, solution cavities in limestone, extent of saprolite, rock color transitions, etc., the weathering zone is limited to a maximum depth of less than 100 ft from the original ground surface.

These observations from the CRBRP excavations are consistent with the CRN Site investigation data regarding depth of weathering and improvement in rock mass discontinuity conditions below a depth of 100 ft, and support the conclusion that continuous open or weathered discontinuities (including bedding planes) are not likely at or below the foundation level.

Alternative Modeling of Weathered Bedding and Fracture Zones

References 1 and 2 provide a PLAXIS finite element 2D model that applies uniform Mohr-Coulomb strength parameters to the inclined site stratigraphy. Using “interface elements” with lower strength values, this model considers a weakened zone along or near geologic formation or member contacts, specifically the Benbolt-Rockdell formation contact and the Eidson-Fleanor member contact, as shown in SSAR Figures 2.5.4-27 and 2.5.4-28. The lower strength is intended to “represent the properties of bedding plane discontinuities (e.g., weathered bedding plane joint zones) and shear fracture zones along stratigraphic contacts for both Site A and Site B” (Reference 2, p. 46). Use of lower strength “interface elements” makes the analysis more

conservative (Reference 2, p. 29, p. 35, p. 43 and p. 76, and SSAR Subsection 2.5.4.13). Modeling results of foundation stability analyses are presented in SSAR Subsection 2.5.4.13. While the site investigation data do not indicate the need to use lowered strength values in modeling a weakened zone, the modeling results validate the use of the GSI in foundation stability analyses as described in the response to RAI Number 02.05.04-02.

Conclusions

SSAR Subsection 2.5.1.2.6.3 describes weathered or fracture zones as typically occurring along bedding planes or fractures and typically represent poor to fair quality rock, consisting of multiple, healed-to-open, slightly-to-highly weathered fractures or bedding planes, some calcite or dolomite filled, with occasional core loss and loss of drilling fluid reported. However, below the uppermost weathered zone (depth of 100 ft or less), rock mass discontinuities (including bedding joints) become tighter, less frequent, and shorter as depth increases. The site investigation data indicates that few bedding joints have identifiable weathering or weakening below the power block foundation level. Therefore, weathering and fractures along bedding planes below the foundation do not result in pre-determined failure surfaces. CRBRP observational data from a grouting program and excavations indicate a rock mass without continuous open or weathered fractures at the foundation level. Therefore, given that GSI is applicable to rock masses with many joint sets (Reference 5), it is concluded that GSI is appropriate to estimate rock mass properties for foundation stability at the CRN Site. An alternative modeling of the discontinuities confirmed this approach.

These conclusions are being added to SSAR Subsections 2.5.1.2.6.3, 2.5.4.2.4.4, and 2.5.4.10.1.2 as provided in the following SSAR markups provided in this Enclosure. The SSAR markups will be incorporated in a future revision of the early site permit application.

References:

1. Rizzo Associates. *Addendum to Non-Proprietary Report Foundation Assessment Clinch River Nuclear Site*, Revision 0, June 15, 2017.

2. Rizzo Associates, *Non-Proprietary Report Foundation Assessment Clinch River Nuclear Site*, Revision 0, June 16, 2017.

3. Howe, R.C., *Geologic Contacts*, Journal of Geoscience Education, v. 45, pp. 133-136, 1997.

4. AMEC Environment and Infrastructure Inc., *Data Report Rev. 4. Geotechnical Exploration and Testing, Clinch River SMR Project, Oak Ridge, Tennessee*. AMEC Project No. 6468-13-1072, October 2014.

5. Hoek, E., T.G. Carter, and M.S. Diederichs, *Quantification of the Geological Strength Index Chart*, 47th U.S. Rock Mechanics/Geomechanics Symposium, San Francisco, CA, 2013.

6. Hoek, E., and P. Marinos, *Predicting tunnel squeezing problems in weak heterogeneous rock masses,* Tunnels and Tunnelling International, Part 1 – November 2000, Part 2 – December, 2000.

7. Hoek, E., C. Carranza-Torres, and B. Corkum, *Hoek-Brown Failure Criterion – 2002 Edition*, Proceedings of the North American Rock Mechanics Symposium and 17th Tunneling Association of Canada Conference, Toronto, Vol. 1, pp. 267–273, 2002.

8. Barton, N.R., and S.C. Bandis, *Review of predictive capabilities of JRC-JCS model in engineering practice*, in Rock Joints, Proceedings International Symposium on Rock Joints, Loen, Norway, (N. Barton and O. Stephansson, eds.), Balkema, Rotterdam, pp. 603-610, 1990.

9. PMC (Project Management Corporation), *Clinch River Breeder Reactor Plant – Preliminary Safety Analysis Report*, Vol. 3, 1982.

10. U.S. Nuclear Regulatory Commission, *Safety Evaluation Report related to the construction of the Clinch River Breeder Reactor Plant*, Docket No. 50-537, NUREG-0968, Vol. 1, Main Report, 1983.

11. Drakulich, N.S., *Geologic mapping of the Clinch River Breeder Reactor Plant excavations*, prepared for the U.S. Department of Energy and CRBRP Project Management Corporation: Stone and Webster Engineering Company, Cherry Hill, NJ, Report No. 12720.50-G(C)-1, 1984.

SSAR Markups

SSAR Subsection 2.5.1.2.6.3 is being revised as indicated. Underlines indicates text to be added.

2.5.1.2.6.3 Fracture Zones

Borings drilled at the CRN Site (Appendix B.1 Reference 2.5.1-214) indicate the presence of weathered or fracture zones within the stratigraphic units. The weathered or fracture zones typically occur along bedding planes or fractures and likely represent early dissolution of the limestone. These zones typically represent poor to fair quality rock consisting of multiple, healed to open, slightly to highly weathered fractures or bedding planes, some calcite or dolomite filled, with occasional core loss and loss of drilling fluid reported. Below the uppermost weathered zone (depth of 100 ft or less), rock mass discontinuities (including bedding joints) become tighter, less frequent, and shorter as depth increases (References 2.5.1-303 and 2.5.1-315). The site investigation data indicate that few bedding fractures have weathering or weakening below the power block foundation level.

The following reference is being added to SSAR Subsection 2.5.1.3. Underlines indicates text to be added.

2.5.1.3 References

2.5.1-315. U.S. Nuclear Regulatory Commission, *Safety Evaluation Report related to the construction of the Clinch River Breeder Reactor Plant*, Docket No. 50-537, NUREG-0968, Vol. 1, Main Report, 1983.

Enclosure 3
Response to NRC RAI Number 6, Question 02.05.04-01

The third paragraph of SSAR Subsection 2.5.4.1.3.1 is being revised as indicated. Underlines indicates text to be added. Strikethroughs indicates text to be deleted.

2.5.4.1.3.1 Discontinuities

Third paragraph

Geologic mapping data of the exposed bedrock surface of the CRBRP excavation are ~~not~~ available and are discussed in Subsection 2.5.1.2.9. ~~but observations~~Observations on the occurrence and orientations of the bedding planes and joints are summarized in a technical paper by Kummerle et al. (Reference 2.5.4-8). Observations during mapping reveal that along the west side of the excavation the bedding planes consistently dip at a steeper angle and the concentration of flatter angles observed in some of the rock core are less frequent. Also, the limestone encountered on the east side of the excavation is reported as thinly bedded while the underlying siltstone is reported as more massive and hard. Fewer high angle joints are also reported than had been assumed for rock excavation design and the joints that were mapped in the thinly bedded limestone are reported to be discontinuous. The dip of the high angle joints are reported to be higher, at or near vertical as opposed to the 70- to 75-degree range assumed for design (Reference 2.5.4-8).

The first paragraph of SSAR Subsection 2.5.4.1.3.3 is being revised as indicated. Underlines indicates text to be added. Strikethroughs indicates text to be deleted.

2.5.4.1.3.3 Weathered and Fracture Zones

A detailed discussion on the weathered/fracture zones encountered in the 100- and 200-series borings at the CRN Site is provided in Subsection ~~2.5.1.2.6.4~~2.5.1.2.6.3. The fracture zones typically occur along bedding planes or fractures and likely represent early dissolution of the limestone. These zones typically represent poor to fair quality rock consisting of multiple, healed to open, slightly to highly weathered fractures or bedding planes, some calcite or dolomite filled, with occasional core loss and loss of drilling fluid reported (Reference 2.5.4-1). A summary of the fracture zones (greater than or equal to approximately 0.9 ft thick [apparent thickness along boring axis]) encountered in the 100- and 200-series is contained in Table 2.5.1-16 and shown on Figure 2.5.1-59. The fracture zones are typically encountered within approximately 50 ft of the ground surface between elevations of approximately 800 and 750 ft and the apparent thickness of the fracture zones ranges from about 1 to 12 ft with an average apparent thickness of about 3 ft.

Enclosure 3
Response to NRC RAI Number 6, Question 02.05.04-01

The second paragraph of SSAR Subsection 2.5.4.2.4.4 is being revised as indicated and a new paragraph is being added after the second paragarph. Underlines indicates text to be added.

2.5.4.2.4.4 Rock Mass Properties

Second paragraph

The properties are developed using the GSI. The application of the GSI classification and Hoek-Brown failure criterion assumes that the rock mass contains several sets of discontinuities that are closely spaced relative to the proposed structure, such that it behaves as a homogeneous and isotropic mass and that a predetermined failure plane does not exist. In other words, while the behavior of the rock mass is controlled by the movement and rotation of the rock blocks separated by intersecting discontinuities, there are no preferred failure directions (Reference 2.5.4-18). The size of the power block excavation is expected to be much larger than the rock blocks that make up the rock mass at the site (Figure 2.5.4-2).

Rock core and geophysical data regarding discontinuities and fractures zones were reviewed for the presence of continuous weathered or fractured zones that provide a predetermined failure plane. As discussed in Subsection 2.5.1.2.6.3, data indicate that weathered or fractured zones are, for the most part, encountered in the uppermost 100 ft. The rock mass below this zone typically is tighter and contains less frequent and less persistent (shorter) discontinuities. Observations from a grouting program conducted within the excavation footprint of the CRBRP and excavation for the CRBRP foundation supports this conclusion (Reference 2.5.4-2, Appendix 2-C, and Reference 2.5.4-61). The grouting program demonstrated very little grout take and the excavation observations reported very little groundwater inflow. Both observations support the conclusion that the discontinuities below the weathered zone are tight, less frequent and shorter and do not result in predetermined failure surfaces.

The last paragraph of SSAR Subsection 2.5.4.2.4.4 is being revised to correct a typographical error as indicated. Underlines indicates text to be added. Strikethroughs indicates text to be deleted.

2.5.4.2.4.4 Rock Mass Properties

Last paragraph

The rock mass deformation moduli estimated using these empirical equations for each of the stratigraphic units are summarized in Table 2.5.4-25. Also in this table for comparison purposes are the moduli obtained from the in situ pressuremeter tests and developed from the low strain Vs data. Rock mass deformation moduli for low strain are frequently overestimated using Vs data and frequently underestimated using in situ pressuremeter test method. This is shown in Table 2.5.4-25 where estimates of the deformation moduli derived from the Vs range from approximately 5000 to 11,400 ksi and from in situ pressuremeter testing range from about 900 to 2400 ksi. Estimates of the rock mass deformation moduli given by Reference 2.5.4-22 (Generalized Hoek-Diederichs method), Reference 2.5.4-19 and Reference 2.5.4-23 for both disturbed (D = 0.7) and undisturbed (D = ~~0.7~~0.0) rock masses generally occur between these ranges and appear to confirm that these empirical methods provide reasonable values for the CRN Site.

Enclosure 3
Response to NRC RAI Number 6, Question 02.05.04-01

SSAR Subsection 2.5.4.10.1.2 is being revised with the following insertion placed after the third paragraph as indicated. Underlines indicates text to be added.

2.5.4.10.1.2 Allowable Bearing Capacity

Third paragraph

A general bearing failure of the foundation is ruled-out due to a net decrease in the bearing pressure at the foundation level. The change in pressure at the foundation level is computed as the assumed new building load (q) minus the existing overburden (σ_o). The amount of unloading (σ_o) is computed for a safety-related structure founded 120 ft below existing grade, resulting in σ_o = 18.7 kilopounds per square foot (ksf). A value of 9 ksf is assumed for the safety-related foundation load, q. Thus, the net change in pressure at the foundation level is expected to be negative – an unloading condition. With a decrease in pressure, general shear failure, including sliding along a predetermined failure plane, such as a bedding plane, is not likely to occur.

Subsection 2.5.1.2.6.3 describes weathered or fracture zones as typically occurring along bedding planes or fractures, and typically represent poor to fair quality rock, consisting of multiple, healed to open, slightly to highly weathered fractures or bedding planes, some calcite or dolomite filled, with occasional core loss and loss of drilling fluid reported. However, below the uppermost weathered zone (depth of 100 ft or less), rock mass discontinuities (including bedding joints) become tighter, less frequent, and shorter as depth increases. The site investigation data indicate that few bedding fractures have weathering or weakening below the power block foundation level. Therefore, weathering and fractures along bedding planes below the foundation are not likely to result in continuous planar discontinuities. GSI is applicable to rock masses with many joint sets (Reference 2.5.4-50), and therefore GSI is appropriate to estimate rock mass properties for foundation stability analysis.

The following reference is being added to SSAR Subsection 2.5.4.14. Underlines indicates text to be added.

2.5.4.14 References

2.5.4-61. U.S. Nuclear Regulatory Commission, *Safety Evaluation Report related to the construction of the Clinch River Breeder Reactor Plant*, Docket No. 50-537, NUREG-0968, Vol. 1, Main Report, 1983.

Enclosure 3
Response to NRC RAI Number 6, Question 02.05.04-01

The titles and notes to the following Figures, added by TVA letter CNL-17-082, are being revised as shown. Underlines indicates text to be added. Strikethroughs indicates text to be deleted.

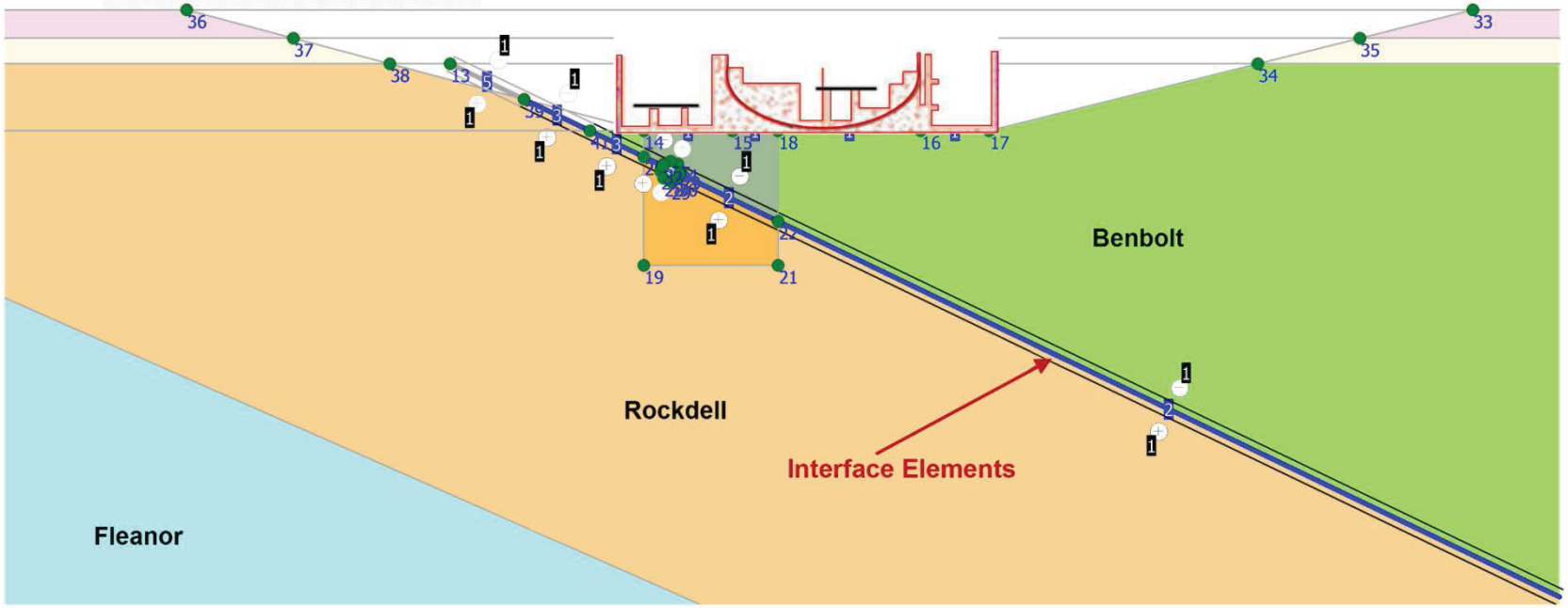

Notes: Reference 2.5.4-59 Figure 2-14
Cavity Diameter: 15 ft
Embedment Depth: 90 ft
Cavity Location: 30 ft Below Edge of Common Basemat
Interface Elements at Formation Contact

Figure ~~2.5.1-27~~2.5.4-27. Finite Element 2D Model of Foundation
Location A, Cross Section: A-A'
~~Cavity Diameter: 15 ft, Embedment Depth: 90 ft~~
~~Cavity Location: 30 ft Below Edge of Common Basemat, Bedding Plane, Shear Joint Interface~~

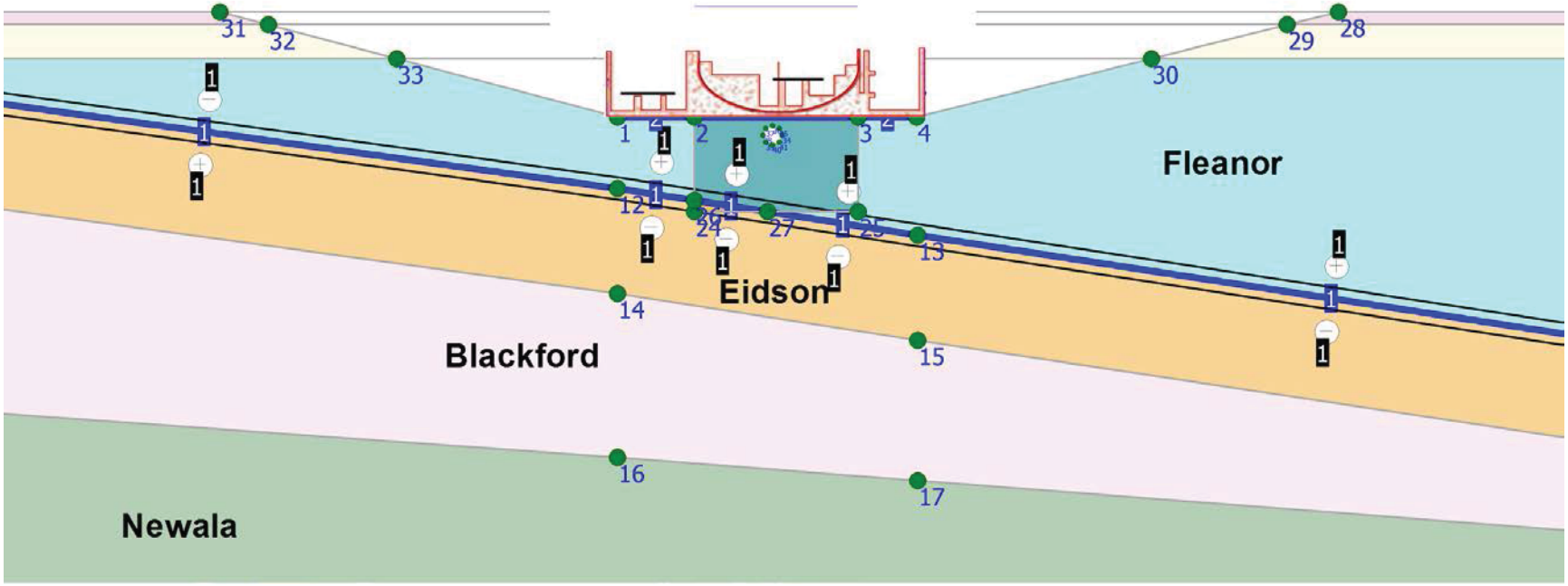

Note: Reference 2.5.4-59 Figure 2-29
Cavity Diameter: 15 ft
Embedment Depth: 90 ft
Cavity Depth: 5 ft Below Foundation
Cavity Location: Center of Common Basemat
Interface Elements at Formation Contact

Figure 2.5.4-28. Finite Element 2D Model of Foundation
Location B, Cross Section: F-F'
~~**Cavity Diameter: 15 ft, Embedment Depth: 90 ft, Cavity Depth: 5 ft Below Foundation, Cavity Location: Center of Common Basemat with Shear Fracture Zone Interface**~~

Enclosure 4

Response to NRC RAI Number 6, Question 02.05.04-02

NRC RAI 02.05.04-02 Question

Bearing capacity and settlement determination

In SSAR (Rev 0) 2.5.4.10 it states that for evaluations of bearing capacity and settlement of rock at the CRN site, each stratigraphic unit within the depth of influence of a respective foundation is considered separately as a single infinite rock layer below the foundation. The basic assumption for the bearing capacity and settlement evaluations simplified the site geologic condition because the actual subsurface of the CRN site consists of multiple inclined layers of different rock formations having some shear and fracture zones. Although the bearing capacity was evaluated using a finite element model (FEM) that takes the site specific geologic characteristics into consideration, and the results are summarized in proposed SSAR markup in Section 2.5.4.13 "Foundation Assessment Model" (TVA CNL-17-082, July 3, 2017), it is not clear whether the FEM results is part of the basis for bearing capacity determination as presented in SSAR Section 2.5.4.10.1 "Bearing Capacity."

To ensure the suitability of the site for future new reactor construction, and stability of subsurface materials and foundations to meet the requirements of 10 CFR 100.23 (d)(4), please (1) discuss all methods used in determination of recommended allowable bearing capacities values in SSAR Section 2.5.4.10.1; (2) justify why the simplified assumptions for site geologic condition and associated methods can be used in evaluation of bearing capacity for the CRN site; and (3) justify why the simplified assumptions and associated methods can be used in evaluation of settlement.

TVA RAI 02.05.04-02 Response

Introduction

Bearing capacity and settlement at the CRN Site are evaluated in SSAR Subsection 2.5.4.10, using a simplified geologic model. This approach was based on results obtained from the site investigation, which indicated that the stratigraphic units beneath the foundations contained similar lithologies, did not exhibit well defined unit boundaries or pre-determined failures surfaces, and exhibited relatively similar strength and stiffness characteristics. At two locations in the power block area, Locations A and B, the evaluations considered each stratigraphic unit within the zone of influence beneath the foundation separately, as a single infinite rock unit. Following the submittal of the CRN Site ESPA Rev. 0, TVA performed confirmatory finite element (FE) modeling, using PLAXIS 2D analysis software, incorporating the inclined layered site stratigraphy. This modeling validated the bearing capacity and settlement results obtained using the simplified geologic model.

Enclosure 4
Response to NRC RAI Number 6, Question 02.05.04-02

The following discussions (1) provide a review of all methods, including FE modeling, used to evaluate bearing capacity; (2) justify the assumptions for the geologic condition and associated methods used for the evaluation of bearing capacity at the CRN Site; and (3) justify why the simplified assumptions and associated methods can be used in evaluation of settlement.

Discussions

(1) A review of methods to evaluate bearing capacity

SSAR Subsection 2.5.4.10.1 presents four methods used to evaluate bearing capacity, which are appropriate for a rock site. The results were screened to select a recommended allowable bearing pressure value of 110 kilopounds per square foot (ksf), as discussed in SSAR Subsection 2.5.4.10.1.2. Three of these methods use empirical equations to derive an allowable bearing capacity using rock mass parameters. Two of these methods, (a) Wyllie (Reference 1) and (b) Kulhawy and Carter (Reference 2) incorporate the Hoek-Brown site-specific rock mass constants (m_i, m_b, s, a), while the third method, (c) US Army Corps of Engineers (Reference 3), uses the site-specific rock mass equivalent friction angle. The fourth method (d) Bowles (Reference 4) uses an empirical relationship based on the rock quality to derive an allowable bearing capacity.

SSAR Subsection 2.5.4.13 provides an alternative (method (e)) to evaluate bearing capacity using a FE model which validates the results presented in SSAR Subsection 2.5.4.10.1.2. This FE model is discussed in detail in References 5 and 6 and is reviewed below.

The Hoek-Brown site-specific rock mass constants were developed considering upper and lower Geologic Strength Index (GSI) values and ground disturbance (D) conditions (D = 0 for undisturbed and D = 0.7 for disturbed ground conditions). The upper and lower GSI values are based on ±1 standard deviation from the average GSI value determined from the subsurface data for each stratigraphic unit. The rock mass properties are summarized in Table 1 (below). The use of GSI in estimating rock mass constants and the application of rock mass properties to the Clinch River Site is appropriate due to the absence of pre-determined failure surfaces below the foundation level as described in the response to RAI 02.05.04-01.

Enclosure 4
Response to NRC RAI Number 6, Question 02.05.04-02

Table 1- Rock Mass Properties

Method / Value	Stratigraphic Unit Name					
	Benbolt Fm. [1]	Rockdell Fm. [1]	Lincolnshire Fm.		Blackford Fm. [3]	Newala Fm. [3]
			Fleanor Mem. [2]	Eidson Mem. [3]		
Rock Mass Modulus of Deformation						
GSI	70	55	65	50	60	70
Generalized Hoek-Diederichs, ksi (D=0.7)	2,059	1,137	1,327	826	1,284	3,849
Gokceoglu et al., ksi (no explicit disturbance factor)	2,048	768	1,477	554	1,065	2,048
Low Strain Elastic Modulus						
Average In Situ Shear Wave Velocity, fps	8,000	9,000	7,200	9,000	8,200	10,800
Low Strain Elastic Modulus, ksi	6,100	7,700	5,000	7,700	6,400	11,400
High Strain Elastic Modulus						
Number of Tests	6	7	9	9	4	10
Average, ksi	6,720	7,463	2,854	6,000	4,953	10,438
Median, ksi	6,890	8,410	2,370	4,980	4,700	11,415
Recommended High Strain Value, ksi	6,700	7,500	2,900	6,000	5,000	10,500
Elastic Modulus SSAR Value, ksi	6,100	7,700	5,000	7,700	6,400	11,400

1) - Rock Unit beneath Location A within zone of influence
2) - Rock Unit beneath Locations A and B within zone of influence
3) - Rock Unit beneath Location B within zone of influence

Abbreviations:
Fm. – Formation
Mem. – Member
fps – feet per second
ksi – kilopounds per square inch

The following is a brief description of the four methods presented in SSAR Subsection 2.5.4.10.1 and the fifth (validation) method presented in SSAR Subsection 2.5.4.13:

(a) Wyllie

Wyllie (Reference 1) evaluates the bearing capacity of a closely fractured or very weak rock based on a failure mechanism similar to the procedure developed by Terzaghi for soil mechanics. Wyllie notes that this is a simplified and conservative analysis which approximates the curved shear failure surface that develops in the foundation materials. The analysis conservatively ignores the confining pressure at the foundation level. The intact rock strength is used directly in the analysis while the degree of fracturing of the rock mass is accounted for using the rock mass parameters, m_b and s.

Wyllie provides the following equation for allowable bearing for a fractured rock mass:

$$q_a = C_{f1} \cdot s^{0.5} \cdot \sigma_{u(r)} \cdot [1 + (m_b \cdot s^{-0.5} + 1)^{0.5}]/FS \qquad \text{Equation 1}$$

where:

q_a = allowable bearing capacity
C_{f1} = shape correction factor based on foundation dimensions, length and width
m_b and s = rock mass constants accounting for the degree of fracturing in the rock mass
$\sigma_{u(r)}$ = unconfined compressive strength of intact rock, alternatively designated σ_{ci}
FS = factor of safety

Wyllie notes that for most loading conditions on sound rock, the FS is in the range of 2 to 3, for which there is little risk of settlement.

(b) Kulhawy and Carter

Alemdag et al. (Reference 7) evaluated the bearing capacity of a jointed rock mass using four different empirical equations incorporating rock mass parameters and concluded that the Wyllie approach, as discussed above, provides conservative results consistent with a similar method suggested by Kulhawy and Carter (Reference 2). The Kulhawy and Carter approach assumes a strip footing (no shape correction factor is accounted for), incorporates the intact rock strength, and accounts for discontinuities in the rock using the rock mass parameters s, a, and m_b in the following equation:

$$q_u = \sigma_{ci} \cdot (s^a + (m_b \cdot s^a + s)^a) \qquad \text{Equation 2}$$

where:

q_u = ultimate bearing capacity
a = rock mass constant accounting for the degree of fracturing in the rock mass

The allowable bearing capacity is calculated by dividing the ultimate capacity by a FS of 3.

(c) US Army Corps of Engineers

The US Army Corps of Engineers Engineering Manual on Rock Foundations (The Manual) (Reference 3) provides bearing capacity analysis methods for four general rock mass conditions: intact, jointed, layered, and highly fractured. Neither intact nor highly fractured conditions reflect the rock mass at the CRN Site. The Manual characterizes a layered rock mass as a rigid rock underlain by a soft highly deformable layer. Given that the stiffness characteristics of the various rock units at the CRN Site are reasonably similar (see rock mass deformation modulus values in Table 1), this rock mass condition also does not reflect the CRN Site. Thus, of the four rock mass conditions, only the jointed rock mass is applicable. Jointed rock mass conditions are subdivided into (i) steeply dipping and closely spaced joints; (ii) steeply dipping and widely spaced joints; and (iii) dipping joints. The Manual describes a dipping joint condition as joints dipping between 20 and 70 degrees with respect to the foundation plane. This applies to the CRN Site which exhibits a dip angle of 33 degrees. Under these conditions, the failure mode of the rock mass is characterized by general shear failure along joints and along an irregular failure surface through the rock mass. The Manual provides the following equation for the evaluation of bearing capacity under these conditions:

$$q_u = 0.5 \cdot \gamma \cdot B \cdot N_\gamma + \gamma \cdot D \cdot N_q \quad \text{Equation 3}$$

where:

D = depth of foundation below ground level
N_γ = bearing capacity factor = $N_{ø}^{0.5} \cdot (N_{ø}^2 - 1)$; for L/B = 2, N_γ is multiplied by 0.90
N_q = bearing capacity factor = $N_{ø}^2$
$N_{ø}$ = bearing capacity factor $= \tan^2 \cdot (45 + \frac{\varphi}{2})$
ø = rock mass equivalent friction angle
B = foundation width
γ = effective unit weight (submerged unit weight if below water table)

Note that Equation 3 does not include a term incorporating rock mass cohesion which may be derived from the rock mass parameters. The Manual notes that cohesion is not incorporated since it cannot be relied upon to provide resistance to failure where failure planes are likely to develop along discontinuities.

The allowable bearing capacity is calculated by dividing the ultimate capacity by a FS of 3.

(d) Bowles

Bowles (Reference 4) notes that geology, rock type, and rock quality are significant parameters that should be used to evaluate allowable bearing capacity. Bowles notes that rock quality is commonly assigned using the rock quality designation (RQD) where RQD is a measure of the quality of the rock mass computed using the following equation:

$$\text{RQD} = \frac{\text{sum of lengths of intact pieces of core} > 4 \text{ in.}}{\text{length of core advance}} \quad \text{Equation 4}$$

Table 2 presents rock quality descriptions based on RQD values.

Table 2 - Rock Quality Designation

RQD	Rock Description
<0.25	Very poor
0.25 - 0.50	Poor
0.50 - 0.75	Fair
0.75 - 0.90	Good
> 0.90	Excellent

Source: Reference 4

At the CRN Site, best estimate RQD values of the rock units ranged from 0.80 to 0.93 (alternatively reported as 80% to 93%), corresponding to quality levels of good to excellent.

Bowles suggests that the allowable bearing capacity of a rock mass can be calculated by applying a FS to the intact unconfined compression strength of the rock where the FS accounts for the rock mass quality. Bowles notes that it is common to use FS from 6 to 10, with the higher values applicable to RQD less than about 0.75.

At the CRN Site, with good to excellent quality rock, a FS of 6 was used.

(e) FE Model

FE modeling using PLAXIS 2D analysis software was conducted to validate the bearing capacity results that were developed using the empirical relationships discussed above. These empirical relationships include some simplified assumptions associated with foundation configuration and site geology, while the FE model incorporates more realistic site-specific configurations and geology. This modeling effort is described in detail in References 5 and 6 and summarized in SSAR Subsection 2.5.4.13. The FE model incorporates the inclined rock units beneath foundations and conservatively includes a weakened interface between rock units. Rock mass properties provided in SSAR Subsection 2.5.4 were used. Foundation loading assumptions were consistent with the values used for the analyses utilizing the empirical relationships.

The failure mode exhibited by the FE modeling results was indicative of a general shear failure, consistent with the assumptions of the empirical approaches. The modeling results provide good agreement with the empirical results.

In summary, four methods were used to evaluate bearing capacity in SSAR Subsection 2.5.4.10.1. These methods considered the various rock units and associated rock mass properties, two foundation disturbance conditions, and two geologic strength conditions. Analyses results gave a range of values for allowable bearing capacity from 48 ksf to 1,697 ksf. A screening of these results yielded a single value of 110 ksf for the allowable bearing capacity value.

A fifth method that used FE modeling considered the inclined layered geology, associated rock mass properties, two embedment depths, and included some conservatism regarding rock unit interface strengths. Results from this analysis are presented in SSAR Subsection 2.5.4.13. As a confirmatory analysis, these results were in good agreement with the results using empirical relationships. Comparing the FE model results with the Bowles method at Location A, the FE model resulted in a value of 147 ksf compared to 149 ksf for the Benbolt Member from Bowles. At Location B, the FE model resulted in a value of 107 ksf compared to a minimum of 108 ksf (Blackford Formation) from Bowles (Reference 6).

The FE modeling results validate the assumptions incorporated into empirical methods used to evaluate bearing capacity, and confirm that these assumptions are appropriate for the CRN Site. They also confirm that the recommended allowable bearing pressure value of 110 ksf is appropriate.

(2) Justify assumptions associated with bearing capacity

SSAR Subsection 2.5.4.10.1 presents the results from the evaluation of bearing capacity at the CRN Site. To evaluate bearing capacity, two assumptions concerning site geology were made. The first of these assumptions pertains to the appropriate use of GSI as described on Page E4-2 of this response and is discussed in detail in the response to RAI 02.05.04-01. The second assumption pertains to the treatment of site stratigraphy. Specifically, each stratigraphic unit beneath the foundation was considered as an infinite half-space when estimating bearing capacity, and the inclined layered stratigraphy beneath the foundation was not considered. These assumptions were based on the observation that the stratigraphic units beneath the foundations contained similar lithologies, did not exhibit well defined unit boundaries, and exhibited relatively similar strength characteristics. Further, the basis of the bearing capacity evaluation was to consider a range of foundation disturbance and geologic strength index (D and GSI, respectively) values for each stratigraphic unit to aid in estimating a representative

design bearing capacity. The observations on lithology, unit boundaries and strength are discussed in the following paragraphs.

At the CRN Site, the stratigraphic units within the zone of influence beneath the foundations at Locations A and B contain similar lithologies ranging from siltstone to limestone. Consistent with their depositional environment, these lithologies are generally transitional and contain interbeds of limestone and siltstone. The CRN Site is primarily underlain by a succession of inclined Upper and Middle Ordovician age rock units of the Chickamauga Group underlain by Lower Ordovician age rocks of the Knox Group. A disconformable contact is located at the top of the Knox Group. With the exception of this regionally extensive disconformity, all contacts between the stratigraphic units are conformable. The rock units of the Chickamauga and Knox Groups exhibit a dip angle of 33 degrees.

The Knox Group immediately underlying the Chickamauga Group at the site consists of the Newala Formation. This formation is described as crystalline dolomite with limestone and dolomitic limestone interbeds. The overlying Chickamauga Group consists mainly of interbedded limestones and siltstone lithofacies. Subdivisions of the Chickamauga Group into the stratigraphic units at the CRN Site follow closely the stratigraphic and lithologic descriptions used by Lee and Ketelle (Reference 8) and the nomenclature established by Hatcher et al. (Reference 9). Stratigraphic units beneath Locations A and B (from oldest to youngest) include the Blackford Formation, Lincolnshire Formation (Eidson and Fleanor Members), Rockdell Formation and Benbolt Formation. The lower portion of the Blackford is identified as dolomitic limestone which transitions to a calcareous siltstone with limestone interbeds. The Eidson Member and the Rockdell are identified as micritic limestone with calcareous siltstone interbeds. The Fleanor Member is identified as calcareous siltstone with micritic limestone interbeds. The Benbolt is identified as limestone with shaley calcareous siltstone interbeds.

Unit stratigraphic boundaries were generally transitional and visibly not well defined. Boundaries provided on the boring logs (Reference 10) were established by the site geologist during the site exploration by comparing the rock core samples to the stratigraphic and lithologic descriptions by Lee and Ketelle (Reference 8). Initially, boundaries were evaluated using overall appearance, color, and gross lithologic composition. When boundaries were difficult to determine and geophysical data were available, natural gamma and conductivity data were used. In borings where no down-hole geophysical testing was available, the field descriptions and core photographs were compared to adjacent borings that did have available geophysical data to establish unit boundaries. Non-geophysical factors such as the presence or absence of chert, the presence or lack of fossils, and the degree of interbedding were also used to establish boundaries. Once the boundaries were established, they were evaluated against regional formation correlations as established by Hatcher et al. (Reference 9).

The strength characteristics of the rocks underlying Locations A and B at the CRN Site were characterized using results from laboratory and in-situ tests as well as rock mass properties. As expected, given that these units have similar lithologies and were deposited in a similar time frame, their strength characteristics are similar. Laboratory testing was conducted on representative core samples of the rock units. These tests included unit weight, specific gravity, and unconfined compression. A summary of results for each rock unit is presented in Table 3 (below). A total of 149 unit weight and specific gravity measurements and 110 unconfined compression tests were conducted. Results show that the rock units of the Chickamauga Group have similar unit weights with an average value of 168 pounds per cubic foot (pcf), while the Newala Formation exhibits higher unit weights with an average value of 175 pcf. Results

from the specific gravity testing corroborate the results for unit weight. Rock units of the Chickamauga Group exhibit similar specific gravity values ranging from 2.68 to 2.70 while the denser Newala Formation of the Knox Group exhibits a specific gravity of about 2.80. Results of unconfined compression tests show similar characteristics, with average strength values reported in the SSAR for the Chickamauga Group being quite consistent, ranging from 4,500 pounds per square inch (psi) in the Blackford Formation to 7,500 psi in the Rockdell Formation. The underlying Newala Formation in the Knox Group has a higher value of 20,000 psi. The consistency of the density and specific gravity values and unconfined strengths in the Chickamauga Group is predictable given the similarities in the lithologies of these rock units.

In-situ shear wave velocity (V_s), normally indicative of rock strength, was measured using the P-S suspension logging method in 28 boreholes across the site. This method provides discrete velocity measurements between the source and two receivers, located 1 meter apart. Table 3 provides a summary of the average V_s values calculated for each rock unit beneath the foundations based on the P-S suspension logging method. All V_s values are in excess of 7,000 feet per second (fps), indicative of strong competent rock. Average V_s values in the Chickamauga Group range from 7,200 fps in the Fleanor Member to 9,000 fps in the Rockdell Formation and Eidson Member. The underlying Newala Formation exhibits an average V_s of 10,800 fps.

Rock mass properties, including rock mass strength, developed using GSI and D values were previously discussed and were summarized in Table 1 (above). A range of values for the Mohr-Coulomb fit friction angle, accounting for the range of GSI and D values, is repeated in Table 3. These values show consistency between the rock units underlying Locations A and B, ranging between 22 and 35 degrees.

Table 3 – Rock Unit Characteristics

Test	Value	Stratigraphic Unit Name						Total No. of Tests
		Benbolt Fm. [1]	Rockdell Fm. [1]	Lincolnshire Fm.		Blackford Fm. [3]	Newala Fm. [3]	
				Fleanor Mem. [2]	Eidson Mem. [3]			
In Situ Shear Wave Velocity	Average, fps	8,000	9,000	7,200	9,000	8,200	10,800	
Unit Weight	Number of Tests	30	20	44	25	15	15	149
	Average, pcf	167.9	167.4	168.2	167.2	166.8	174.0	
	Median, pcf	168	168	168	167	167	176	
	SSAR, pcf	168	168	168	168	168	175	
Specific Gravity	Number of Tests	30	20	44	25	15	15	149
	Average	2.70	2.69	2.70	2.69	2.68	2.79	
	Median	2.70	2.69	2.70	2.69	2.68	2.82	
	SSAR	2.70	2.69	2.70	2.69	2.68	2.80	
Unconfined Compression	Number of Tests	17	16	30	23	9	15	110
	Average, psi	6,173	8,714	5,423	8,032	6,236	21,421	
	Median, psi	6,300	7,550	5,315	7,390	4,770	21,790	
	SSAR, psi	6,200	7,500	5,000	7,000	4,500	20,000	
Mohr-Coulomb Fit, friction angle (deg.)	Range of ϕ	28 - 33	24 - 35	26 - 35	22 - 35	24 - 33	31 - 35	

1) - Rock Unit beneath Location A within zone of influence
2) - Rock Unit beneath Locations A and B within zone of influence
3) - Rock Unit beneath Location B within zone of influence
Abbreviations:
Fm. – Formation
Mem. – Member
fps – feet per second
pcf – pounds per cubic foot
psi – pounds per square inch

In summary, the use of a simplified geologic model to evaluate bearing capacity is appropriate due to (1) the similarities of rock units underlying the foundations at Locations A and B based on visual observation of rock cores, in-situ testing, and laboratory testing, and (2) the stratigraphic boundaries of these rock units being generally transitional and visibly not well defined, i.e., no

identifiable weak zones at the stratum boundaries. This model considers each stratigraphic unit beneath the foundation as an infinite half-space and the bearing capacity for each unit is evaluated. For each stratigraphic unit, a range of GSI values and different disturbance factors was considered. From the results a recommended bearing capacity value was selected. The appropriateness of the simplified geologic model and bearing capacity evaluation was confirmed with the use of a FE model as discussed above in response to Item (1) and as presented in SSAR Subsection 2.5.4.13.

(3) Justify assumptions associated with evaluation of settlement

SSAR Subsection 2.5.4.10.2 presents the results from the evaluation of settlement and heave at the CRN Site. Regardless of the methodology used, computed settlement and heave values are negligible. Similar to the evaluation of bearing capacity as discussed in response to Item (2), the evaluation of settlement utilizes the simplified geologic model. This model considers settlement of each stratigraphic unit within the zone of influence beneath the foundation, with each unit acting as an infinite half-space. The inclined layered stratigraphy beneath the foundation is not considered. As demonstrated above for bearing capacity, these assumptions are appropriate because the stratigraphic units beneath the foundations contain similar lithologies, do not exhibit well defined unit boundaries, and exhibit similar strength characteristics. The following paragraphs discuss the similarities of the stiffness characteristics of the various stratigraphic units, with these similarities further supporting the use of a simplified model to evaluate settlement.

The stiffness characteristics of the rocks underlying Locations A and B at the CRN Site were evaluated using rock mass deformation moduli based on empirical relationships incorporating rock mass parameters and elastic modulus values. Two methods were used to calculate the rock mass deformation modulus values and estimate settlement. These methods are designated:

a. Generalized Hoek-Diederichs (Reference 11)
b. Gokceoglu et al. (Reference 12)

Rock mass deformation modulus values were calculated for a range of GSI values and two disturbance conditions (D = 0.0 and D = 0.7), similar to the evaluation of rock mass strength for bearing capacity. For illustration purposes, results considering the lower GSI value and larger disturbance factor for each of the underlying rock units are presented in Table 4 (below).

Rock unit stiffness was also evaluated considering the elastic modulus values (E) derived from in-situ V_s measurements and measured in laboratory unconfined compression tests. As previously discussed, in-situ V_s measurements were taken in 28 boreholes across the site. Generally, for strong, competent rock, the shear and elastic modulus are the same at both small strains (V_s measurements) and large strains (laboratory test measurements). The low-strain elastic modulus (E_L) is calculated using the following relationships:

$$E_L = G_L \cdot [2 \cdot (1+\mu)] \quad \text{Equation 5}$$

where:

μ = Poisson's ratio
G_L = low-strain shear modulus

and $$G_L = (\gamma/g) \cdot V_s^2 \quad \text{Equation 6}$$

where:

γ = unit weight
g = acceleration due to gravity

A summary of the calculated low-strain elastic modulus values for the various stratigraphic units is provided in Table 4. High-strain elastic modulus values were determined from laboratory testing using ASTM D7012 (Reference 13). A summary of these results is presented in Table 4. Generally, high-strain and low-strain elastic modulus results compare favorably. Recommended elastic modulus values reported in SSAR Subsection 2.5.4 are included in Table 4.

Low-strain modulus values derived from in-situ V_s data are usually higher than the computed rock mass modulus values. This can be seen in Table 4 where the low-strain modulus values consistently exceed the rock mass modulus values. Table 4 also illustrates the relative similarity of modulus values between stratigraphic units, particularly within the Chickamauga Group. This similarity in stiffness is one basis for using a simplified geologic model to evaluate settlement.

Table 4 – Stiffness Characteristics

Method / Value	Stratigraphic Unit Name					
	Benbolt Fm. [1]	Rockdell Fm. [1]	Lincolnshire Fm.		Blackford Fm. [3]	Newala Fm. [3]
			Fleanor Mem. [2]	Eidson Mem. [3]		
Rock Mass Modulus of Deformation						
GSI	70	55	65	50	60	70
Generalized Hoek-Diederichs, ksi (D=0.7)	2,059	1,137	1,327	826	1,284	3,849
Gokceoglu et al., ksi (no explicit disturbance factor)	2,048	768	1,477	554	1,065	2,048
Low Strain Elastic Modulus						
Average In Situ Shear Wave Velocity, fps	8,000	9,000	7,200	9,000	8,200	10,800
Low Strain Elastic Modulus, ksi	6,100	7,700	5,000	7,700	6,400	11,400
High Strain Elastic Modulus						
Number of Tests	6	7	9	9	4	10
Average, ksi	6,720	7,463	2,854	6,000	4,953	10,438
Median, ksi	6,890	8,410	2,370	4,980	4,700	11,415
Recommended High Strain Value, ksi	6,700	7,500	2,900	6,000	5,000	10,500
Elastic Modulus SSAR Value, ksi	6,100	7,700	5,000	7,700	6,400	11,400

1) - Rock Unit beneath Location A within zone of influence
2) - Rock Unit beneath Locations A and B within zone of influence
3) - Rock Unit beneath Location B within zone of influence
Abbreviations:
Fm. – Formation
Mem. – Member
fps – feet per second
ksi – kilopounds per square inch

Settlement (δ) beneath Locations A and B was calculated with rock mass deformation moduli using the following equation from Reference 3:

$$\delta = \frac{1.12 \cdot q \cdot B \cdot (1-\mu^2) \cdot (\frac{L}{B})^{0.5}}{E_d} \qquad \text{Equation 7}$$

where:

E_d = rock mass modulus of deformation (E_{rm})
q = applied foundation load
L = foundation length
B = foundation width
μ = Poisson's ratio

Note that Equation 7 provides a solution for a flexible foundation. The settlement of a rigid foundation is calculated by multiplying the Equation 7 solution by a reduction factor. Reduction factors of 0.78 and 0.82, based on L/B as provided in Reference 3, were evaluated.

Settlement was calculated using rock mass modulus values derived using the two methods previously discussed as well as using upper and lower GSI values and disturbance factors of D = 0.0 and D = 0.7. Two structures were analyzed, with L ≈ 300 feet and B ≈ 220 feet and 115 feet. Results gave estimated settlement ranging from 0.01 inch to 0.28 inch.

FE modeling was also used to evaluate settlement. The model was initially set up to consider the presence of a void beneath the foundation and the impact on the foundation as discussed in SSAR Subsection 2.5.4.13. The foundation configuration in the FE model differed somewhat from the configurations considered in SSAR Subsection 2.5.4.10.2 but was reasonably similar. This FE model considered the inclined layered geology, associated rock mass properties, and conservatively included a weakened interface between rock units. Modeling results gave settlement values ranging from 0.06 inch to 0.13 inch. (Reference 5)

A comparison of settlement results using the simplified geologic model and the inclined layered geology as provided in the FE model shows good agreement, confirming that initial assumptions regarding the simplified geologic model are appropriate for the CRN Site.

Revisions to SSAR Subsections 2.5.4.10, 2.5.4.10.1, and 2.5.4.13 are provided in the following SSAR markups provided in this Enclosure. SSAR Subsection 2.5.4.10 is being revised to summarize the basis for utilizing a simplified geologic model for the site and the appropriateness of this model for the evaluation of bearing capacity and settlement. The revision also identifies that a FE model is presented in SSAR Subsection 2.5.4.13 as validation of these results. SSAR Subsection 2.5.4.10.1 is being revised to move the last paragraph up to SSAR Subsection 2.5.4.10. SSAR Subsection 2.5.4.13 is being revised to clarify that the FE analysis is provided as a validation of the results in SSAR Subsection 2.5.4.10. The SSAR markups will be incorporated in a future revision of the early site permit application.

References:

1. Wyllie, D.C., “Foundations on Rock,” 2nd Edition, E&FN Spon, Abingdon, 1999.

2. Kulhawy, F.H., and J.P. Carter, “Settlement and Bearing Capacity of Foundations on Rock Masses and Socketed Foundations in Rock Masses,” F.G. Bell (ed.). Engineering in Rock Masses, Butterworth-Heinemann, Oxford, 231-245, 1992.

3. U.S. Army Corps of Engineers, “Rock Foundations,” EM 1110-1-2908, 1994.

4. Bowles, J.E., “Foundation Analysis and Design,” 3rd Edition, McGraw-Hill Inc., New York, 1982.

5. Rizzo Associates, “Non-Proprietary Report Foundation Assessment, Clinch River Nuclear Site,” Foundation Assessment, Revision 0, June 16, 2017.

6. Rizzo Associates, “Addendum to Non-Proprietary Report Foundation Assessment, Clinch River Nuclear Site,” Foundation Assessment, Revision 0, June 15, 2017.

7. Alemdag, S., Z. Gurocak, P. Zolanki, and N. Zaman, “Estimation of Bearing Capacity of Basalts at the Atasu Dam Site, Turkey,” Bulletin of Engineering Geology and the Environment, Vol. 67: 79-85, 2007.

8. Lee, R. R. and R. H. Ketelle, “Subsurface Geology of the Chickamauga Group at Oak Ridge National Laboratory,” ORNL/TM-10749, Oak Ridge National Laboratory, 1988.

9. Hatcher, R.D., Jr., P.J. Lemiszki, R.B. Dreier, R.H. Ketelle, R.R. Lee, D.A. Lietzke, W.M. McMaster, J.L. Foreman, and S.Y. Lee, “Status Report on the Geology of the Oak Ridge Reservation, Oak Ridge National Laboratory,” ORNL/TM-12074, Environmental Sciences Division Publication 3860: pp. 29–39, 1992.

10. AMEC Environment and Infrastructure Inc., “Data Report Rev. 4. Geotechnical Exploration and Testing, Clinch River SMR Project, Oak Ridge, Tennessee,” AMEC Project No. 6468-13-1072, October 16, 2014.

11. RocData Software, Version 4.014, RocScience, Inc, Toronto, Ontario.

12. Gokceoglu, C., H. Sonmez, and A. Kayabasi, “Predicting the Deformation Moduli of Rock Masses,” International Journal of Rock Mechanics and Mining Sciences, Vol 40: pp. 701-710, 2003.

13. ASTM D7012, “Standard Test Method for Compressive Strength and Elastic Moduli of Intact Rock Core Specimens under Varying States of Stress and Temperatures,” ASTM International, West Conshohocken, PA, 2014.

Enclosure 4
Response to NRC RAI Number 6, Question 02.05.04-02

SSAR Markups

SSAR Subsection 2.5.4.10 is being revised as indicated. Underlines indicates text to be added.

2.5.4.10 Static and Dynamic Stability

This section presents the evaluation of static and dynamic stability of safety-related structures including bearing capacity, heave, settlement, and lateral earth pressures in the power block area at the CRN Site. The geologic features at the site are summarized in Subsection 2.5.4.1 (described in detail in Subsection 2.5.1) and the subsurface investigation and laboratory testing programs are described in Subsection 2.5.4.3. Description of the subsurface materials, including the engineering properties of the existing fill/residual soil and bedrock units, are described in Subsection 2.5.4.2.

Subsection 2.5.4.1.1 describes the stratigraphy at the site and Figure 2.5.4-2 presents a cross-section through the power block area. The site is underlain with a succession of stratigraphic units that generally strike N63°E with a dip angle of 33 degrees. Rocks belonging to the Knox Group outcrop to the northwest and progressively younger rocks belonging to the Chickamauga Group outcrop to the southeast. The stratigraphic units within the power block area include, from northwest to southeast, the Newala Formation, the Blackford Formation, the Eidson and Fleanor Members, the Rockdell Formation, and the Benbolt Formation. The average thickness of these units is presented in Table 2.5.4-1.

Subsection 2.5.4.1.3 describes the discontinuities, shear-fracture zones and weathered/fracture zones encountered in the stratigraphic units. These discontinuities may impact the stability of foundations and are accounted for by considering the effect of rock mass properties on the performance of the foundations. Subsection 2.5.4.2.4.4 describes the rock mass strength and deformation properties.

Overlying the dipping bedrock units, a layer of weathered rock and existing fill/residual soil is encountered at the CRN Site. These materials are described in Subsection 2.5.4.2.4. Existing site grades vary within the power block area with an average elevation of approximately 810 ft. The finished grade elevation is 821 ft. Compacted granular fill is used to replace weathered rock, residual soil, and existing fill beneath structures and to establish finished grade.

Due to the dipping strata at the CRN Site, the stratigraphic units underlying the power block area vary depending on location. At the northwest end of the power block area the Newala Formation outcrops at the ground surface while to the southeast, this formation is estimated to be well over 1000 ft below the ground surface. For this reason, the two specific locations in the power block area, Location A and Location B are evaluated for static and dynamic stability of safety-related structures with a foundation embedment of 138 ft below finished grade (El. 683 ft). The existing ground surface elevation at Location A is approximately 800 ft, while the elevation at Location B is approximately 810 ft.

Reference 2.5.4-50 provides a GSI chart that suggests rock with a rock quality designation (RQD) above 80 percent is representative of intact or massive rock and is controlled by material properties rather than discontinuities. As noted in Table 2.5.4-21, the average RQD values of the bedrock at the CRN Site range from 80 to 93 percent. Nevertheless, the application of the GSI classification and the Hoek-Brown relationship is based on observations that the rock mass

contains several sets of discontinuities that are closely spaced relative to the dimensions of the proposed structure and a predetermined failure plane does not exist. The applicability of GSI in rock mass characterization is discussed in Subsection 2.5.4.2.4.4.

A simplified stratigraphic model along with empirical relationships are used for the evaluation of bearing capacity in Subsections 2.5.4.10.1.1 and 2.5.4.10.1.2, and settlement and heave in Subsection 2.5.4.10.2. The stratigraphy underlying the CRN Site consists of an inclined layered system of alternating siltstones and limestones. The similarity of the engineering properties of these rock units, in both strength and stiffness, suggests that, for evaluation purposes, the individual rock units may be considered separately to develop a range of results. Material properties of intact rock and rock mass properties based on GSI are considered in evaluating bearing capacity and settlement and heave. A finite element model, presented in Subsection 2.5.4.13, is used to validate the assumptions and empirical relationships used.

The last paragraph of SSAR Subsection 2.5.4.10.1 is deleted as indicated. Strikethroughs indicates text to be deleted.

2.5.4.10.1 Bearing Capacity

Last paragraph

~~Reference 2.5.4-50 provides a GSI chart which suggests rock with a rock quality designation (RQD) above 80 percent is representative of intact or massive rock and is controlled by material properties rather than discontinuities. As noted in Table 2.5.4-21, the average RQD values of the bedrock at the CRN Site range from 80 to 93 percent. However, the application of the GSI classification and the Hoek-Brown relationship is based on observation that the rock mass contains several sets of discontinuities that are closely spaced relative to the dimensions of the proposed structure. For the evaluation of bearing capacity in Subsections 2.5.4.10.1.1 and 2.5.4.10.1.2, empirical relationships using material properties of intact rock and rock mass properties based on GSI are considered.~~

Enclosure 4
Response to NRC RAI Number 6, Question 02.05.04-02

The last paragraph of SSAR Subsection 2.5.4.13 is being revised as indicated. Underlines indicates text to be added. Strikethroughs indicates text to be deleted.

In addition to the karst evaluation performed in the PLAXIS 2D analysis, an additional analysis of the site bearing capacity was performed for Locations A and B at 80 and 138 foot depths. This finite-element analysis is provided to confirm the validity of the simplified model used for bearing capacity and settlement in Subsection 2.5.4.10 ~~included a finite-element model to determine the ultimate bearing capacity at the CRN Site~~. The analysis is provided in Reference 2.5.4-60. The ultimate bearing capacity for the CRN Site is high, ranging from 320 kips per square foot to 526 kips per square foot for the sections and embedment depths evaluated. The ultimate bearing capacity for Location A is estimated as 441 kips per square foot, and the ultimate bearing capacity for Location B is estimated as 320 kips per square foot, Geometry modifications were made to allow the PLAXIS model to be more consistent with the bearing capacity calculations presented in Subsection 2.5.4.10.1.2 and Table 2.5.4-27. When a factor of safety of 3 is considered to determine the allowable bearing capacity, the values from this analysis compare very well with the previously performed allowable bearing capacity analysis as presented in Subsection 2.5.4.10. For Location A, the PLAXIS bearing capacity is 147 kips per square foot as compared to the SSAR bearing capacity of 149 kips per square foot. For Location B, the PLAXIS bearing capacity is 107 kips per square foot as compared to the SSAR bearing capacity of 108 kips per square foot. In general, the comparison of these two methodologies and the subsequent results demonstrates a reasonable agreement for the allowable bearing capacity.